Algebraic Representations in Computer-Aided Design for complEx Shapes

ARCADES Book

Extended abstracts of PhD Theses of the ARCADES fellows

ATHENS
December 31, 2019

Introduction

ARCADES is a European project funded under the H2020-MSCA-ITN-2015 call and is part of the Marie Sklodowska-Curie Actions — Innovative Training Networks (ITN) funding scheme (Grant agreement No: 675789). ARCADES aims at disrupting the traditional paradigm in Computer-Aided Design (CAD) by exploiting cutting-edge research in mathematics and algorithm design. Geometry is now a critical tool in a large number of key applications; somewhat surprisingly, however, several approaches of the CAD industry are outdated, and 3D geometry processing is becoming increasingly the weak link. This is alarming in sectors where CAD faces new challenges arising from fast point acquisition, big data, and mobile computing, but also in robotics, simulation, animation, fabrication and manufacturing, where CAD strives to address crucial societal and market needs. The challenge taken up by ARCADES is to invert the trend of CAD industry lagging behind mathematical breakthroughs and to build the next generation of CAD software based on strong foundations from algebraic geometry, differential geometry, scientific computing, and algorithm design. Our game-changing methods lead to real-time modellers for architectural geometry and visualisation, to isogeometric and design-through-analysis software for shape optimisation, and marine design & hydrodynamics, and to tools for motion design, robot kinematics, path planning, and control of machining tools.

ARCADES trains 13 ESR fellows; this book collects their project results. It contains the extended abstracts of the PhD Theses of the fellows that have completed their doctoral studies before December 31st. The book will be updated regularly to eventually include the abstracts of the theses of all 13 ARCADES ESRs. The full theses will be available upon completion at http://arcades-network.eu/index.php/publications/

Project facts
Duration: 48 Months (01/2016 — 12/2019)
Project Coordinator: Ioannis Z. Emiris (emiris AT athena-innovation.gr)
Technical Coordinator: Christos Konaxis (ckonaxis AT di.uoa.gr)
Educational Committee: Laurent Busé (Chair) (Laurent.Buse AT inria.fr), Panagiotis Kaklis, Carlos D'Andrea, Georg Muntingh

Acknowledgements

This project has received funding by the European Union's Horizon 2020 research and innovation programme under the Marie Skłodowska-Curie grant agreement No 675789.

Marie Skłodowska-Curie
Actions

Contents

List of Figures

List of Tables

Chapter 1

Clément Laroche: Compact and efficient implicit representations

We are interested in the representation of geometric objects, such as surfaces and curves. The diversity of what can be called a geometric object depends on what kind of operations should be possible on these objects and the degree of complexity we consent to them. Using algebra proved to be a very powerful way of dealing with a broad range of objects; thus most of the geometric objects studied here are algebraic objects. If we sometimes refer to non-algebraic objects, it is always with the prospective of constructing an algebraic structure out of them.

In order to describe a geometric object, one can use the vocabulary of the school, combining straight lines, circles and other simple shapes. One can also draw up a list of all the points belonging to the object, up to a given precision. It is also possible to describe an object by the use of discriminating properties satisfied by its points (e.g. being invariant by a given transformation) or its coordinates (e.g. satisfying some equation). Or, more abstractly, one can give properties of the object, such as its size, compactness, connected components, description of its boundaries, genus, curvature, etc.

When it comes to computers, all these geometric representations can be useful in some context. The main difference with abstract representations is that the quantity of information required to describe an object within a given representation method must be finite. For example, Bézier curves and patches form a basis of simple shapes that can be combined to have more complex shapes in Computer-Aided Geometric Design (CAGD). Even simpler: triangular surfaces can be combined in order to for a triangular mesh of a 3D object, which is useful in Computer-Aided Engineering (CAE). In bitmap imaging, objects are described pixel by pixel. In Algebraic Geometry, a variety is the zero set of polynomial or rational equation(s). And so on…

A representation is thus a list of informations (typically numbers) while a representation method determines how these informations should be interpreted. More theoretically, a (computer) representation method is a partial surjection from $\mathbb{N}^{\mathbb{N}}$ to a set of representable objects by that representation method. This set of representable objects can have at most

the cardinality of the continuum, which is large enough for representing most of geometric objects one can think of. For instance, the sets of (graphs of) polynomials, analytic functions over the unit complex disc or even continuous functions over a compact subset of $\mathbb{R}^n$ are all representable sets (see [1, 2] for more details about these representation methods of very large spaces). However, the set of (graphs of) real-valued functions is not representable. In our algebraic framework, we restrain ourselves mostly to representation methods of algebraic varieties, the geometric objects we can build out of them and the operations that can be done with them.

Of course, an object representable by one representation method may not be representable by another method. An elliptic curve, for instance, can be described as the zero set of a degree 3 polynomial but it cannot be described using Bezier curves or even rational parameterisations. On the other hand, a large set of objects can be represented using several different representation methods. An important problem is then to be able to pass from a representation to another. The difficulty to convert an object from one representation to another relates with the diversity of these representation methods.

Among these representation methods, two kinds are of greater importance for us:

- Parametric representations, taking one or several parameters as input and a point of the object as output. Typically, a parametric representation of an algebraic object is a birational map between a projective space and that object.

- Implicit representations, taking a point of the ambient space as input and outputting whether that point belongs to the object or not. Typically, an implicit representation is a set of polynomials that simultaneously vanish on the object.

We sometimes refer to the *generic case*. Unless explicitly stated otherwise, a property is said to hold for the generic case when it holds for a (topologically) dense subset of objects and also holds (probabilistically) almost surely when a random object is picked with a dense probability measure. In algebraic geometry, these two notions of density and almost certainty coincide most of the time, provided that the underlying field is algebraically closed (typically, $\mathbb{K} = \mathbb{C}$).

The work presented in my thesis is about describing interesting ways to represent algebraic objects with a focus on implicit representations and developing algorithms to switch from a representation to another with a focus on implicitisation, i.e. algorithms that output an implicit representation.

The author has followed PhD studies at the National and Kapodistrian University of Athens in Greece in the framework of the project ARCADES funded by the Marie Skłodowska-Curie Actions. As part of these studies, the author has spent 3 months at the research center SINTEF in Olso, Norway, and 4 months at the research center RISC Software GmbH in Hagenberg, Austria. In both occasions, work has been done collaboratively with the local research teams.

In chapter 2 of the thesis, basic tools are presented. Gröbner bases and resultants are the main tools when it comes to implicitisation algorithms. We present both, with an emphasise on resultants because the algorithms on the subsequent chapters rely on them rather than on Gröbner bases. Moreover, a C++ implementation of a sparse resultant algorithm has been developed by the author based on an existing Maple implementation. We also present a very basic interpolation matrix that can be built for varieties of any (co)dimension.

In chapter 3 of the thesis, a new implicitisation algorithm for a special kind of 3D objects is developed. Two implicitisation algorithms used in the industry are also presented.

In chapter 4 of the thesis, a new implicitisation algorithm of varieties of codimension strictly greater than 1 is developed. While several implicitisation algorithms fare better on hypersurfaces, this one on the contrary is better suited for varieties of high codimension. The idea behind that algorithm comes from the theory of Chow forms which is also presented there. That chapter is based on the article [3].

In chapter 5, a new matrix-based implicitisation algorithm is developed. This algorithm relies on syzygies and chain complexes. It provides a very strong link between parametric and implicit representations, allowing to reverse the map between the parametric and ambient spaces through the implicit matrix. That chapter is based on the article [4].

In chapter 6, we compare different implicitisation methods, outlining the advantages and drawbacks of each one. Since most representations can more useful than the others depending on the situation (a fact that is true when comparing parametric and implicit representations but even when comparing implicit representations amongst themselves), it is a necessary work to be done.

Chapter 2

Yairon Cid Ruiz: Blow-up algebras in Algebra, Geometry and Combinatorics

The primary topic of this thesis lies at the crossroads of Commutative Algebra and its interactions with Algebraic Geometry and Combinatorics. It is mainly focused around the following themes:

I Defining equations of blow-up algebras.

II Study of rational maps via blow-up algebras.

III Asymptotic properties of the powers of edge ideals of graphs.

We are primarily interested in questions that arise in geometrical or combinatorial contexts and try to understand how their possible answers manifest in various algebraic structures or invariants. There is a particular algebraic object, the Rees algebra (or blow-up algebra), that appears in many constructions of Commutative Algebra, Algebraic Geometry, Geometric Modeling, Computer Aided Geometric Design and Combinatorics. The workhorse and main topic of this doctoral dissertation has been the study of this algebra under various situations.

The Rees algebra was introduced in the field of Commutative Algebra in the famous paper [121]. Since then, it has become a central and fundamental object with numerous applications. The study of this algebra has been so fruitful that it is difficult to single out particular results or papers, instead we refer the reader to the books [144] and [146] to wit the "landscape of blow-up algebras".

From a geometrical point of view, the Rees algebra corresponds with the bi-homogeneous coordinate ring of two fundamental objects: the blow-up of a projective variety along a subvariety and the graph of a rational map between projective varieties (see [66, §II.7]). Therefore, the importance of finding the defining equations of the Rees algebra is probably beyond argument. This is a problem of tall order that has occupied commutative algebraists and algebraic geometers, and despite an extensive effort (see [14, 20, 34–36, 38, 39, 78, 100, 103–105, 108, 113, 143]), it remains open even in the case of polynomial rings in two variables. In [29], Chapter 2 of this dissertation,

we use the theory of D-modules to describe the defining ideal of the Rees algebra in the case of a parametrization of a plane curve.

The study of rational and birational maps is classical in the literature from both an algebraic and geometric point of view, and it goes back to the work of Cremona [41], at least. A relatively new idea, probably first used in [80], is to look at the syzygies of the base ideal of a rational map to determine birationality. This algebraic method for studying rational maps has now become an active research topic (see [16, 46, 51, 67, 68, 102, 119, 124, 129]). In a joint work with Busé and D'Andrea [22], Chapter 3 of this dissertation, we introduce a new algebra that we call the saturated special fiber ring, which turns out to be an important tool to analyze the degree of a rational map. Later, in [30], Chapter 4 of this dissertation, we compute the multiplicity of this new algebra in the case of perfect ideals of height two, which, in particular, provides an effective method to determine the degree of a rational map having those ideals as base ideal.

Often a good tactic to approach a challenging problem is to go all the way up to a generic case and then find sufficient conditions for the specialization to keep some of the main features of the former. The procedure depends on taking a dramatic number of variables to allow modifying the given data into a generic shape, and usually receives the name of specialization. This method is seemingly due to Kronecker and was quite successful in the hands of Hurwitz ([86]) in establishing a new elegant theory of elimination and resultants. More recent instances where specialization is used are, e.g., [84], [85], [141], [132]. In a joint work with Simis [33], Chapter 5 of this dissertation, we consider the behavior of the degree of a rational map under specialization of the coefficients of the defining linear system.

The Rees algebra of the edge ideal of a graph is a well studied object (see [54, 56, 136, 147–150]), that relates combinatorial properties of a graph with algebraic invariants of the powers of its edge ideal. For the Rees algebra of the edge ideal of a bipartite graph, in [31], Chapter 6 of this dissertation, we compute the universal Gröbner basis of its defining equations and its total Castelnuovo-Mumford regularity as a bigraded algebra.

It is a celebrated result that the regularity of the powers of a homogeneous ideal is asymptotically a linear function (see [42, 99]). Considerable efforts have been put forth to understand the form of this asymptotic linear function in the case of edge ideals (see [3, 4, 8–10, 62, 90]). In a joint work with Jafari, Picone and Nemati [32], Chapter 7 of this dissertation, for bicyclic graphs, i.e. graphs containing exactly two cycles, we characterize the regularity of its edge ideal in terms of the induced matching number and determine the previous asymptotic linear function in special cases.

The basic outline of this thesis is as follows. In Chapter 1, we recall some preliminary results and definitions to be used along this work. Then, the thesis is divided in three different parts. The first part corresponds with the theme *"*$\boxed{\text{I}}$ *Defining equations of blow-up algebras"* and consists of Chapter 2. The second part corresponds with the theme *"*$\boxed{\text{II}}$ *Study of rational maps via blow-up algebras"* and consists of Chapter 3, Chapter 4 and Chapter 5. The third part corresponds with the theme *"*$\boxed{\text{III}}$ *Asymptotic properties of the powers of edge ideals of graphs"* and consists of Chapter

6 and Chapter 7. The common thread and main tool in the three parts of this thesis is the use of blow-up algebras.

In the subsequent sections of the introduction, we describe the motivations, organization, and main contributions and results of this dissertation.

I Defining equations of blow-up algebras

Let $\mathbb{F}$ be a field of characteristic zero, R be the polynomial ring $R = \mathbb{F}[x_1, x_2]$, and $I = (f_1, f_2, f_3) \subset R$ be a height two ideal minimally generated by three homogeneous polynomials of the same degree d. The Rees algebra of I is defined as $\mathcal{R}(I) = R[It] = \bigoplus_{i=0}^{\infty} I^i t^i$. We can see $\mathcal{R}(I)$ as a quotient of the polynomial ring $S = R[T_1, T_2, T_3]$ via the map

$$S = R[T_1, T_2, T_3] \xrightarrow{\psi} \mathcal{R}(I), \quad \psi(T_i) = f_i t.$$

Of particular interest are the defining equations of the Rees algebra $\mathcal{R}(I)$, that is, the kernel $\mathcal{I} = \mathrm{Ker}(\psi)$ of this map ψ. A large number of works have been done to determine the equations of the Rees algebra, and the problem has been studied by algebraic geometers and commutative algebraists under various conditions (see e.g. [144] and the references therein). In recent years, a lot of attention has been given to find the minimal generators of the equations of the Rees algebra for an ideal in a polynomial ring (see e.g. [20, 34–36, 38, 39, 79, 100, 103–105, 108]), partly inspired by new connections with Geometric Modeling. Despite this extensive effort, even in the "simple" case studied in Chapter 2, the problem of finding the minimal generators of $\mathcal{I}$ remains open.

By the Hilbert-Burch Theorem (see e.g. [47, Theorem 20.15]) we know that the presentation of I is of the form

$$0 \to R(-d-\mu) \oplus R(-2d+\mu) \xrightarrow{\varphi} R(-d)^3 \xrightarrow{[f_1,f_2,f_3]} I \to 0,$$

and I is generated by the 2×2-minors of φ; we may assume that $0 < \mu \leqslant d - \mu$. The symmetric algebra of I can easily be described as a quotient of S by using the presentation of I. The defining equations of the symmetric algebra are given by

$$[g_1, g_2] = [T_1, T_2, T_3] \cdot \varphi,$$

and so we have $\mathrm{Sym}(I) \cong S/(g_1, g_2)$. There is an important relation between $\mathrm{Sym}(I)$ and $\mathcal{R}(I)$ in the form of the following canonical exact sequence

$$0 \to \mathcal{K} \to \mathrm{Sym}(I) \xrightarrow{\alpha} \mathcal{R}(I) \to 0.$$

Here we have $\mathcal{K} = \mathcal{I}/(g_1, g_2)$, which allows us to take $\mathcal{K}$ as the object of study.

The main novelty of Chapter 2 is the use of D-modules to find different descriptions of $\mathcal{K}$. In Chapter 2, we prove that $\mathcal{K}$ can be described as the solution set of a system of differential equations,

that the whole bigraded structure of $\mathcal{K}$ is characterized by the integral roots of certain b-functions, and that certain de Rham cohomology groups can give partial information about $\mathcal{K}$.

The polynomial ring S is bigraded with $\operatorname{bideg}(T_i) = (1,0)$ and $\operatorname{bideg}(x_i) = (0,1)$, and $\mathcal{K}$, $\operatorname{Sym}(I)$ and $\mathcal{R}(I)$ have natural structures of bigraded S-modules. Let $\mathcal{T}$ be the polynomial ring $\mathcal{T} = A_2(\mathbb{F})[T_1, T_2, T_3]$ over the Weyl algebra $A_2(\mathbb{F})$ and consider the differential operators $L_1 = \mathcal{F}(g_1)$ and $L_2 = \mathcal{F}(g_2)$ by applying the Fourier transform to g_1 and g_2 (see Definition 2.14).

The first main result of Chapter 2 gives that $\mathcal{K}$ can be described by solving a system of differential equations.

Theorem A (Theorem 2.18)**.** *Let* $I \subset R = \mathbb{F}[x_1, x_2]$ *be a height two ideal minimally generated by three homogeneous polynomials of the same degree* d*, and* g_1 *and* g_2 *be the defining equations of the symmetric algebra of* I*. Let* $L_1 = \mathcal{F}(g_1)$ *and* $L_2 = \mathcal{F}(g_2)$ *be the Fourier transform of* g_1 *and* g_2*, respectively. Then, we have the following isomorphism of bigraded* S*-modules*

$$\mathcal{K} \cong \operatorname{Sol}\Big(L_1, L_2; S\Big)_{\mathcal{F}}(-2, -d+2),$$

where $\operatorname{Sol}(L_1, L_2; S) = \{h \in S \mid L_1 \bullet h = 0$ *and* $L_2 \bullet h = 0\}$ *and the subscript-*$\mathcal{F}$ *denotes the twisting by the Fourier transform (Section 2.2).*

Since g_1 and g_2 generate all the linear part of $\mathcal{I}$ (the syzygies of I) and $\mathcal{K} = \mathcal{I}/(g_1, g_2)$, then we have $\mathcal{K}_{p,*} = 0$ for all $p < 2$. As an application of Theorem A we give a complete characterization of the graded structure of each R-module $\mathcal{K}_{p,*}$ ($p \geqslant 2$) in terms of the integral roots of certain b-functions (Definition 2.26).

Theorem B (Theorem 2.31)**.** *Let* $I \subset R = \mathbb{F}[x_1, x_2]$ *be as in Theorem A. Then, for each integer* $p \geqslant 2$ *there exists a nonzero* b*-function* $b_p(s)$*, and we have a relation between the graded structure of* $\mathcal{K}_{p,*}$ *and the integral roots of* $b_p(s)$ *given in the following equivalence*

$$\mathcal{K}_{p,q} \neq 0 \qquad \Longleftrightarrow \qquad b_p(-d+2+q) = 0.$$

Even more, we have that these are the only possible roots of $b_p(s)$*, that is*

$$b_p(s) = \prod_{\{q \in \mathbb{Z} \mid \mathcal{K}_{p,q} \neq 0\}} (s + d - 2 - q).$$

Theorem B is interesting for us in the sense that it gives a tool for deducing information about $\mathcal{K}$, but on the other hand, from a D-module point of view it is worthy to note that it describes the b-function of a family of holonomic D-modules like those in Setup 2.21.

Let U be the polynomial ring $U = \mathbb{F}[T_1, T_2, T_2]$.

In the last main result of Chapter 2, we change the role of L_1 and L_2, more specifically, instead of having them as operators we place them in a quotient. We make this change by means of a duality proven in Theorem 2.32, which allows us to establish an isomorphism of graded U-modules

between $\mathcal{K}$ and a certain de Rham cohomology group. In particular, this isomorphism could give an alternative way to compute or estimate the dimension $\dim_{\mathbb{F}}(\mathcal{K}_{p,*})$ of each $\mathcal{K}_{p,*}$ regarded as finite dimensional $\mathbb{F}$-vector space (see Corollary 2.6).

Theorem C (Theorem 2.37)**.** *Let* $I \subset R = \mathbb{F}[x_1, x_2]$, L_1 *and* L_2 *be as in Theorem A, and let* Q *be the left* $\mathcal{T}$*-module* $Q = \mathcal{T}/\mathcal{T}(L_1, L_2)$*. Then, we have the following isomorphism of graded* U*-modules*

$$\mathcal{K} \cong H^0_{dR}(Q) = \{w \in Q \mid \partial_1 \bullet w = 0 \text{ and } \partial_2 \bullet w = 0\}.$$

In particular, for any integer p *we have an isomorphism of* $\mathbb{F}$*-vector spaces*

$$\mathcal{K}_{p,*} \cong H^0_{dR}(Q_p) = \{w \in Q_p \mid \partial_1 \bullet w = 0 \text{ and } \partial_2 \bullet w = 0\}.$$

The basic outline of Chapter 2 is as follows. In Section 2.1, we prove Theorem 2.5. In Section 2.2, we make a translation of our problem into the theory of D-modules and we prove Theorem A. In Section 2.3, we prove Theorem B. In Section 2.4, we prove Theorem C. In Section 2.5, we present a script in *Macaulay2* [60] that can compute each b-function $b_p(s)$ from Theorem B, and using it we effectively recover the bigraded structure of $\mathcal{K}$ for a couple of examples.

II Study of rational maps via blow-up algebras

Questions and results concerning the degree and birationality of rational maps are classical in the literature from both an algebraic and geometric point of view. These problems have been extensively studied since the work of Cremona [41] in 1863 and are still very active research topics (see e.g. [2, 45, 46, 64, 80, 129] and the references therein). However, there seems to be very few results and no general theory available for multi-graded rational maps, i.e. maps that are defined by a collection of multi-homogeneous polynomials over a subvariety of a product of projective spaces. At the same time, there is an increasing interest in those maps, for both theoretic and applied purposes (see e.g. [15, 16, 77, 127, 128]).

In Chapter 3, we give formulas and effective sharp bounds for the degree of multi-graded rational maps and provide some effective criteria for birationality in terms of their algebraic and geometric properties. Sometimes we also improve known results in the single-graded case. Our approach is based on the study of blow-up algebras, including syzygies, of the ideal generated by the defining polynomials of a rational map, which is called the base ideal of the map. This idea goes back to [80] and since then a large amount of papers has blossomed in this direction (see e.g. [16, 46, 51, 67, 68, 102, 119, 124, 129]).

One of the main contributions in Chapter 3 is the introduction of a new algebra that we call the *saturated special fiber ring* (see Definition 3.3). The fact that saturation plays a key role in this kind of problems has already been observed in previous works in the single-graded setting (see [67], [92, Theorem 3.1], [118, Proposition 1.2]). Based on that, we define this new algebra by taking certain multi-graded parts of the saturation of all the powers of the base ideal. It can be seen as an

extension of the more classical special fiber ring. We show that this new algebra turns out to be a fundamental ingredient for computing the degree of a rational map (see Theorem 3.4), emphasizing in this way that saturation has actually a prominent role to control the degree and birationality of a rational map. In particular, it allows us to prove a new general numerical formula (see Corollary 3.12) from which the degree of a rational map can be extracted. Another interesting feature of the saturated special fiber ring is its relation with the j-multiplicity of an ideal (see Lemma 3.10).

Next, we refine the above results for rational maps whose base locus is zero-dimensional. We begin by providing a purely algebraic proof (see Theorem 3.16) of the classical degree formula in intersection theory (see e.g. [55, Section 4.4]) adapted to our setting. Then, we investigate the properties that can be extracted if the syzygies of the base ideal of a rational map are used. This idea amounts to use the symmetric algebra to approximate the Rees algebra and it allows us to obtain sharp upper bounds (see Theorem 3.21) for the degree of multi-graded rational maps. Some applications to more specific cases of multi-projective rational maps (see Proposition 3.24) and projective rational maps (see Theorem 3.34) are also discussed, with the goal of providing efficient birationality criteria in the low-degree cases (see e.g. Proposition 3.27, Theorem 3.28 and Proposition 3.35).

The problem of detecting whether a rational map is birational has attracted a lot of attention in the past thirty years. A typical example is the class of Cremona maps (i.e. birational) in the projective plane that have been studied extensively (see e.g. [2]). Obviously, the computation of the degree of a rational map yields a way of testing its birationality. Nevertheless, this approach is not very efficient and various techniques have been developed in order to improve it and to obtain finer properties of birational maps. Among these specific techniques, the Jacobian dual criterion introduced and fully developed in [46, 124, 129] has its own interest. In Section 3.3, we extend the theory of the Jacobian dual criterion to the multi-graded setting (see Theorem 3.39) and derive some consequences where the syzygies of the base ideal are used instead of the higher-order equations of the Rees algebra (see Theorem 3.44).

In Chapter 3, we also study the particular class of plane rational maps whose base ideal is saturated and has a syzygy of degree one. In this setting, we provide a very effective birationality criterion (see Theorem 3.59) and a complete description of the equations of the associated Rees algebra (see Theorem 3.57).

Now, we fix a basic notation in order to describe some results of Chapter 3 in more detail.

Let $\Bbbk$ be a field, $X_1 \subset \mathbb{P}^{r_1}_{\Bbbk}, X_2 \subset \mathbb{P}^{r_2}_{\Bbbk}, \ldots, X_m \subset \mathbb{P}^{r_m}_{\Bbbk}$ and $Y \subset \mathbb{P}^{s}_{\Bbbk}$ be integral projective varieties over $\Bbbk$. For $i = 1, \ldots, m$, the homogeneous coordinate ring of X_i is denoted by $A_i = \Bbbk[\mathbf{x_i}]/\mathfrak{a}_i = \Bbbk[x_{i,0}, x_{i,1}, \ldots, x_{i,r_i}]/\mathfrak{a}_i$, and $S = \Bbbk[y_0, y_1, \ldots, y_s]/\mathfrak{b}$ stands for the homogeneous coordinate ring of Y. Set $R = A_1 \otimes_{\Bbbk} A_2 \otimes_{\Bbbk} \cdots \otimes_{\Bbbk} A_m \cong \Bbbk[\mathbf{x}]/(\mathfrak{a}_1, \mathfrak{a}_2, \ldots, \mathfrak{a}_m)$. Let

$$\mathcal{F} : X = X_1 \times_{\Bbbk} X_2 \times_{\Bbbk} \cdots \times_{\Bbbk} X_m \dashrightarrow Y \subset \mathbb{P}^{s}_{\Bbbk}$$

be a dominant rational map defined by $s+1$ multi-homogeneous elements $\mathbf{f} = \{f_0, f_1, \ldots, f_s\} \subset R$ of the same multi-degree $\mathbf{d} = (d_1, d_2, \ldots, d_m)$. We also assume that X is an integral variety.

The degree of the dominant rational map $\mathcal{F} : X = X_1 \times_{\Bbbk} X_2 \times_{\Bbbk} \cdots \times_{\Bbbk} X_m \dashrightarrow Y$ is defined as $\deg(\mathcal{F}) = [K(X) : K(Y)]$, where $K(X)$ and $K(Y)$ represent the fields of rational functions of X and Y, respectively.

The ring $R = A_1 \otimes_{\Bbbk} A_2 \otimes_{\Bbbk} \cdots \otimes_{\Bbbk} A_m$ has a natural multi-grading given by

$$R = \bigoplus_{(j_1,\ldots,j_m)\in\mathbb{Z}^m} (A_1)_{j_1} \otimes_{\Bbbk} (A_2)_{j_2} \otimes_{\Bbbk} \cdots \otimes_{\Bbbk} (A_m)_{j_m}.$$

Let $\mathfrak{N}$ be the multi-homogeneous irrelevant ideal of R, that is

$$\mathfrak{N} = \bigoplus_{j_1>0,\ldots,j_m>0} R_{j_1,\ldots,j_m}.$$

For an arbitrary ideal $J \subset R$, let J^{sat} be the ideal $(J\colon \mathfrak{N}^{\infty})$. Let T be the multi-Veronese subring which is given by the standard graded $\Bbbk$-algebra

$$T = \Bbbk[R_{\mathbf{d}}] = \bigoplus_{n=0}^{\infty} R_{n\cdot\mathbf{d}}.$$

The homogeneous coordinate ring S is often called the special fiber ring in the literature, and using the canonical graded homomorphism associated to $\mathcal{F}$ we obtain the identification

$$S \cong \Bbbk[f_0, f_1, \ldots, f_s] = \Bbbk[I_{\mathbf{d}}] = \bigoplus_{n=0}^{\infty} [I^n]_{n\cdot\mathbf{d}}$$

In Chapter 3, we define the following saturated version of S.

Definition D (Definition 3.3)**.** *The saturated special fiber ring of* I *is the graded* S*-algebra*

$$\widetilde{\mathcal{F}_R(I)} = \bigoplus_{n=0}^{\infty} \left[(I^n)^{\text{sat}}\right]_{n\cdot\mathbf{d}}.$$

Interestingly, the algebra $\widetilde{\mathcal{F}_R(I)}$ turns out to be finitely generated as an S-module.

The main result of Chapter 3 is given in the following theorem. It shows, for instance, that a comparison between the multiplicities of S and $\widetilde{\mathcal{F}_R(I)}$ yields the degree of $\mathcal{F}$, and that under some conditions $\mathcal{F}$ is birational if and only if $S = \widetilde{\mathcal{F}_R(I)}$.

Theorem E (Theorem 3.4)**.** *Let* $\mathcal{F} : X = X_1 \times_{\Bbbk} X_2 \times_{\Bbbk} \cdots \times_{\Bbbk} X_m \dashrightarrow Y$ *be a dominant rational map. If* $\dim(Y) = \dim(X)$*, then we have the following commutative diagram*

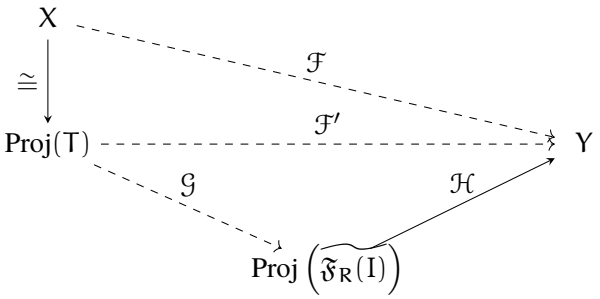

where the maps $\mathcal{F}' : \mathrm{Proj}(T) \dashrightarrow Y$, $\mathcal{G} : \mathrm{Proj}(T) \dashrightarrow \mathrm{Proj}\left(\widetilde{\mathfrak{F}_R(I)}\right)$ *and* $\mathcal{H} : \mathrm{Proj}\left(\widetilde{\mathfrak{F}_R(I)}\right) \to Y$ *are induced from the inclusions* $S \hookrightarrow T$, $\widetilde{\mathfrak{F}_R(I)} \hookrightarrow T$ *and* $S \hookrightarrow \widetilde{\mathfrak{F}_R(I)}$, *respectively.*

Also, the statements below are satisfied:

(i) $\mathcal{H} : \mathrm{Proj}\left(\widetilde{\mathfrak{F}_R(I)}\right) \to Y$ *is a finite morphism with* $\deg(\mathcal{F}) = \deg(\mathcal{H})$.

(ii) $\mathcal{G}$ *is a birational map.*

(iii) $e\left(\widetilde{\mathfrak{F}_R(I)}\right) = \deg(\mathcal{F}) \cdot e(S)$, *where* $e(-)$ *stands for multiplicity.*

(iv) Under the additional condition of S *being integrally closed, then* $\mathcal{F}$ *is birational if and only if* $\widetilde{\mathfrak{F}_R(I)} = S$.

We remark that all the hypotheses and consequences in the previous theorem do not depend on the characteristic of the field $\Bbbk$. By applying Theorem E, we give formulas and effective sharp bounds for the degree of multi-graded rational maps and provide some criteria for birationality in terms of their algebraic and geometric properties.

An example of such a criterion for birationality is the following characterization of birational maps from a multi-projective space onto a projective space, which in particular applies to Cremona transformations.

Corollary F (Proposition 3.24)**.** *Let* $\mathcal{F} : \mathbb{P}^{r_1}_{\Bbbk} \times_{\Bbbk} \mathbb{P}^{r_2}_{\Bbbk} \times_{\Bbbk} \cdots \times_{\Bbbk} \mathbb{P}^{r_m}_{\Bbbk} \dashrightarrow \mathbb{P}^{\delta}_{\Bbbk}$ *be a dominant rational map with* $r_1 + r_2 + \ldots + r_m = \delta$. *Then, the map* $\mathcal{F}$ *is birational if and only if for all* $n \geqslant 1$ *we have*

$$[I^n]_{n\cdot\mathbf{d}} = \left[(I^n)^{\mathrm{sat}}\right]_{n\cdot\mathbf{d}}.$$

An example of such an upper bound for the degree of a rational map is the following.

Proposition G (Proposition 3.35)**.** *Let* $\mathcal{F} : \mathbb{P}^2_{\Bbbk} \dashrightarrow \mathbb{P}^2_{\Bbbk}$ *be a dominant rational map with a dimension* 1 *base ideal* I *minimally generated by three polynomials of degree* d. *Then, the following statements hold:*

(i) $\deg(\mathcal{F}) \leqslant \frac{(d-1)(d-2)}{2} + \dim_{\Bbbk}\left([I^{\mathrm{sat}}/I]_d\right) + 1$.

(ii) If I *is of linear type and* $d \leqslant 3$*, then* $\deg(\mathcal{F}) = \frac{(d-1)(d-2)}{2} + \dim_{\Bbbk}\left([I^{sat}/I]_d\right) + 1$.

Now, we briefly describe the relation of the saturated special fiber ring with the j-multiplicity of an ideal. The j-multiplicity of an ideal was introduced in [1] and serves as a generalization of the Hilbert-Samuel multiplicity for non $\mathfrak{m}$-primary ideals. It has applications in intersection theory (see [53]), and the problem of finding formulas for it has been addressed in several papers (see e.g. [91, 92, 114, 120]). Let A be a standard graded $\Bbbk$-algebra of dimension $\delta + 1$ which is an integral domain. Let $\mathfrak{m}$ be its maximal irrelevant ideal $\mathfrak{m} = A_+$ and let J^{sat} be $(J\colon \mathfrak{m}^\infty)$ for any ideal $J \subset A$. For a non necessarily $\mathfrak{m}$-primary ideal $J \subset A$ its j-multiplicity is given by

$$j(J) = \delta! \lim_{n\to\infty} \frac{\dim_{\Bbbk}\left(H^0_{\mathfrak{m}}\left(J^n/J^{n+1}\right)\right)}{n^\delta}.$$

Lemma H (Lemma 3.10)**.** *Let* $J \subset A$ *be a homogeneous ideal equally generated in degree* d*. Suppose* J *has maximal analytic spread* $\ell(J) = \delta + 1$*. Then, we have the equality*

$$j(J) = d \cdot e\left(\widetilde{\mathfrak{F}_A(J)}\right),$$

where $\widetilde{\mathfrak{F}_A(J)} = \bigoplus_{n=0}^{\infty}\left[(J^n)^{sat}\right]_{nd}$ *is the saturated special fiber ring of* J.

Another sought interest of Chapter 3 is to develop a multi-graded version of the Jacobian dual criterion of [46]. This remarkable criterion gives necessary and sufficient conditions to test the birationality of a rational map, and, also, it should be noted that does not depend on the characteristic of the field $\Bbbk$. Additionally, when the map is birational, we can get the inverse map.

The following theorem contains a multi-graded version of the Jacobian dual criterion.

Theorem I (Theorem 3.39)**.** *Let* $\mathcal{F} : X_1 \times_{\Bbbk} X_2 \times_{\Bbbk} \cdots \times_{\Bbbk} X_m \dashrightarrow Y$ *be a dominant rational map. Let* ψ *and* ψ_i *for* $1 \leqslant i \leqslant m$ *be the Jacobian dual matrices of Notation 3.37. Then, the following three conditions are equivalent:*

(i) $\mathcal{F}$ *is birational.*

(ii) $\operatorname{rank}_S(\psi_i \otimes_{\Bbbk[y]} S) = r_i$ *for each* $i = 1, \ldots, m$.

(iii) $\operatorname{rank}_S(\psi \otimes_{\Bbbk[y]} S) = r_1 + r_2 + \cdots + r_m$.

In addition, if $\mathcal{F}$ *is birational then its inverse is of the form* $\mathcal{G} : Y \dashrightarrow X_1 \times_{\Bbbk} X_2 \times_{\Bbbk} \cdots \times_{\Bbbk} X_m$*, where each map* $Y \dashrightarrow X_i$ *is given by the signed ordered maximal minors of an* $r_i \times (r_i + 1)$ *submatrix of* ψ_i *of rank* r_i.

The basic outline of Chapter 3 is as follows. In Section 3.1, we introduce the saturated special fiber ring and we prove Theorem E. In Section 3.2, we study rational maps with a finite base locus. In Section 3.3, we extend the Jacobian dual criterion to the multi-graded setting and we prove Theorem I. In Section 3.4, we study a particular class of plane rational maps.

The case of perfect ideals of height two

In Chapter 4, we compute the multiplicity of the saturated special fiber ring for a general family of perfect ideals of height two. Interestingly, this formula is equal to an elementary symmetric polynomial in terms of the degrees of the syzygies of the ideal. As two simple corollaries, for this class of ideals, we obtain a closed formula for the j-multiplicity and an effective method for determining the degree and birationality of rational maps defined by homogeneous generators of these ideals.

Let $\Bbbk$ be a field, R be the polynomial ring $R = \Bbbk[x_0, x_1, \dots x_r]$, and $\mathfrak{m}$ be the maximal irrelevant ideal $\mathfrak{m} = (x_0, x_1, \dots, x_r)$. Let $I \subset R$ be a perfect ideal of height two which is minimally generated by $s+1$ forms $\{f_0, f_1, \dots, f_s\}$ of the same degree d.

To determine the multiplicity of $\widetilde{\mathcal{F}_R(I)}$, we need to study the first local cohomology module of the Rees algebra of I, and for this we assume the condition G_{r+1}. The condition G_{r+1} means that $\mu(I_\mathfrak{p}) \leqslant \dim(R_\mathfrak{p})$ for every non-maximal ideal $\mathfrak{p} \in V(I) \subset \operatorname{Spec}(R)$, where $\mu(I_\mathfrak{p})$ denotes the minimal number of generators of $I_\mathfrak{p}$. To study the Rees algebra one usually tries to reduce the problem in terms of the symmetric algebra, the assumption of G_{r+1} is important in making possible this reduction. After reducing the problem in terms of the symmetric algebra, we consider certain Koszul complex that provides an approximate resolution (see e.g. [101], [24]) of the symmetric algebra, and which permits us to compute the Hilbert series of $\widetilde{\mathcal{F}_R(I)}$. By pursuing this general approach, we obtain the following theorem which is the main result of Chapter 4.

Theorem J (Theorem 4.8)**.** *Let* $I \subset R = \Bbbk[x_0, x_1, \dots, x_r]$ *be a homogeneous ideal minimally generated by* $s+1$ *forms* $\{f_0, f_1, \dots, f_s\}$ *of the same degree* d*, where* $s \geqslant r$*. Suppose the following two conditions:*

(i) I *is perfect of height two with Hilbert-Burch resolution of the form*

$$0 \to \bigoplus_{i=1}^{s} R(-d-\mu_i) \to R(-d)^{s+1} \to I \to 0.$$

(ii) I *satisfies the condition* G_{r+1}*, that is* $\mu(I_\mathfrak{p}) \leqslant \dim(R_\mathfrak{p})$ *for all* $\mathfrak{p} \in V(I) \subset \operatorname{Spec}(R)$ *such that* $\operatorname{ht}(\mathfrak{p}) < r+1$.

Then, the multiplicity of the saturated special fiber ring $\widetilde{\mathcal{F}_R(I)}$ *of* I *is given by*

$$e\left(\widetilde{\mathcal{F}_R(I)}\right) = e_r(\mu_1, \mu_2, \dots, \mu_s),$$

where $e_r(\mu_1, \mu_2, \dots, \mu_s)$ *represents the* r*-th elementary symmetric polynomial*

$$e_r(\mu_1, \mu_2, \dots, \mu_s) = \sum_{1 \leqslant j_1 < j_2 < \cdots < j_r \leqslant s} \mu_{j_1}\mu_{j_2}\cdots\mu_{j_r}.$$

The following result gives a formula for the j-multiplicity of a whole family of ideals.

Corollary K (Corollary 4.10)**.** *Assume all the hypotheses and notations of Theorem J. Then, the* j*-multiplicity of* I *is given by*

$$j(I) = d \cdot e_r(\mu_1, \mu_2, \ldots, \mu_s).$$

In the second application of Theorem J, we study the degree of a rational map $\mathcal{F} : \mathbb{P}^r_{\Bbbk} \dashrightarrow \mathbb{P}^s_{\Bbbk}$ defined by the tuple of forms $\{f_0, f_1, \ldots, f_s\}$. We show that the product of the degree of $\mathcal{F}$ and the degree of the image of $\mathcal{F}$ is equal to $e_r(\mu_1, \ldots, \mu_s)$. From this we can determine the degree of a rational map by just computing the degree of the image, and conversely, the degree of the map gives us the degree of the image. In particular, we obtain that the map is birational if and only if the degree of the image is the maximum possible.

Corollary L (Corollary 4.11)**.** *Assume all the hypotheses and notations of Theorem J. Let* $\mathcal{F}$ *be the rational map* $\mathcal{F} : \mathbb{P}^r_{\Bbbk} \dashrightarrow \mathbb{P}^s_{\Bbbk}$ *given by*

$$(x_0 : \cdots : x_r) \mapsto \big(f_0(x_0, \ldots, x_r) : \cdots : f_s(x_0, \ldots, x_r)\big),$$

and $Y \subset \mathbb{P}^s_{\Bbbk}$ *be the closure of the image of* $\mathcal{F}$*. Then, the following two statements hold:*

(i) $\deg(\mathcal{F}) \cdot \deg_{\mathbb{P}^s_{\Bbbk}}(Y) = e_r(\mu_1, \mu_2, \ldots, \mu_s)$.

(ii) $\mathcal{F}$ *is birational onto its image if and only if* $\deg_{\mathbb{P}^s_{\Bbbk}}(Y) = e_r(\mu_1, \mu_2, \ldots, \mu_s)$.

The basic outline of Chapter 4 is as follows. In Section 4.1, we prove Theorem J. In Section 4.2, we study rational maps whose base ideals satisfy the conditions of Theorem J.

Specialization of rational maps

The overall goal of Chapter 5 is to obtain bounds for the degree of a rational map in terms of the main features of its base ideal. In order that this objective stays within a reasonable limitation, we focus on rational maps whose source and target are projective varieties.

Now, to become more precise we should rather talk about projective schemes as source and target of the envisaged rational maps. The commonly sought interest is the case of projective schemes over a field (typically, but not necessarily, algebraically closed).

One tactic that has often worked is to go all the way up to a generic case and then find sufficient conditions for the specialization to keep some of the main features of the former. The procedure depends on taking a dramatic number of variables to allow modifying the given data into a generic shape. The method is seemingly due to Kronecker and was quite successful in the hands of Hurwitz ([86]) in establishing a new elegant theory of elimination and resultants. Of a more recent crop, we have, e.g., [84], [85], [141], [132].

In a related way, we have the notion of when an ideal specializes modulo a regular sequence: given an ideal $I \subset R$ in a ring, we say that I specializes with respect to a sequence of elements

$\{a_1, \ldots, a_n\} \subset R$ if the latter is a regular sequence both on R and on R/I. A tall question in this regard is to find conditions under which the defining ideal of some well-known rings – such as the Rees ring or the associated graded ring of an ideal (see, e.g., [49], [97]) – specialize with respect to a given sequence of elements. Often, at best we can only describe some obstructions to this sort of procedure, normally in terms of the kernel of the specialization map.

The core of Chapter 5 can be said to lie in between the two ideas of specialization as applied to the situation of rational maps between projective schemes and their related ideal-theoretic objects.

It so happens that at the level of the generic situation the coefficients live in a polynomial ring A over a field, not anymore on a field. This entails the need to consider rational maps defined by linear systems over the ring A, that is, rational maps with source $\mathbb{P}^r_A$. As it turns out, it is not exceedingly more complicated to consider rational maps with source an integral closed subscheme of $\mathbb{P}^r_A$.

Much to our surprise a complete such theory, with all the required details that include the ideal-theoretic transcription, is not easily available. For this reason, the first part of Chapter 5 deals with such details with an eye for the ideal-theoretic behavior concealed in or related to the geometric facts. A tall order in these considerations will be a so-called *relative fiber cone* that mimics the notion of a fiber cone (or special fiber ring; see Remark 5.4) in the classical environment over a field – this terminology is slightly misleading as the notion is introduced in algebraic language, associated to the concept of a Rees algebra rather than to the geometric version (blowup); however, we will draw on both the algebraic and the geometric versions.

Another concept dealt with is the *relative saturated fiber cone*, an object perhaps better understood in terms of global sections of a suitable sheaf of rings. In Chapter 5, the saturated special fiber ring (Definition D) is extended to the case when the coefficients belong to a Noetherian integral domain of finite Krull dimension. It contains the relative fiber cone as a subalgebra and plays a role in rational maps (see Theorem 5.25).

With the introduction of these considerations, we will be equipped to tackle the problem of specialization of rational maps, which is the main objective of Chapter 5. The neat application so far is to the multiplicity of the saturated fiber cone and to the degree of a rational map defined by the maximal minors of a homogeneous $(r+1) \times r$ matrix, when in both situations we assume that the coefficient ring A is a polynomial ring over a field of characteristic zero.

Another important result is that under a suitable general specialization of the coefficients, we show that the degree of the rational map never decreases, that the degree of the corresponding image never increases, but that the product of the two previous degrees remains constant.

Next there is a more detailed summary of the main results of Chapter 5.

Here we assume that the ground ring is a polynomial ring $A = \Bbbk[z_1, \ldots, z_m]$ over a field $\Bbbk$. In this setting we specialize the variables z_i to elements of $\Bbbk$. Thus, we consider a maximal ideal of the form $\mathfrak{n} = (z_1 - \alpha_1, \ldots, z_m - \alpha_m)$ where $\alpha_i \in \Bbbk$. Since clearly $\Bbbk \cong A/\mathfrak{n}$, the A-module structure of $\Bbbk$ is given via the homomorphism $A \twoheadrightarrow A/\mathfrak{n} \cong \Bbbk$. We take a standard graded polynomial ring $R = A[x_0, \ldots, x_r]$ ($[R]_0 = A$) and a tuple of forms $\{g_0, \ldots, g_s\} \subset R$ of the same positive degree.

Let $\{\overline{g_0}, \dots, \overline{g_s}\} \subset R/\mathfrak{n}R$ denote the corresponding tuple of forms in $R/\mathfrak{n}R \cong \Bbbk[x_0, \dots, x_r]$ where $\overline{g_i}$ is the image of g_i under the canonical homomorphism $R \twoheadrightarrow R/\mathfrak{n}R$.

Consider the rational maps

$$\mathcal{G} : \mathbb{P}^r_A \dashrightarrow \mathbb{P}^s_A \quad \text{and} \quad \mathcal{g} : \mathbb{P}^r_\Bbbk \dashrightarrow \mathbb{P}^s_\Bbbk$$

determined by the tuples of forms $\{g_0, \dots, g_s\}$ and $\{\overline{g_0}, \dots, \overline{g_s}\}$, respectively.

The main target is finding conditions under which the degree $\deg(\mathcal{g})$ of $\mathcal{g}$ can be bounded above or below by the degree $\deg(\mathcal{G})$ of $\mathcal{G}$. Set $\mathcal{I} = (g_0, \dots, g_s) \subset R$ and $I = (\overline{g_0}, \dots, \overline{g_s}) \subset R/\mathfrak{n}R$. Let $\mathcal{E}(\mathcal{I})$ be the exceptional divisor of the blow-up of $\mathbb{P}^r_A$ along $\mathcal{I}$. A bit surprisingly, having a grip on the dimension of the scheme $\mathcal{E}(\mathcal{I}) \times_A \Bbbk$ is the main condition to determine whether $\deg(\mathcal{g}) \leqslant \deg(\mathcal{G})$ or $\deg(\mathcal{g}) \geqslant \deg(\mathcal{G})$. The main result in this direction is the following theorem.

Theorem M (Theorem 5.44)**.** *Suppose that both $\mathcal{G}$ and $\mathcal{g}$ are generically finite.*

(i) Assume that the following conditions hold:

- *(a)* $\operatorname{Proj}(A[\mathbf{g}])$ *is a normal scheme.*
- *(b)* $\dim(\mathcal{E}(\mathcal{I}) \times_A \Bbbk) \leqslant r$.
- *(c)* $\Bbbk$ *is a field of characteristic zero.*

Then

$$\deg(\mathcal{g}) \leqslant \deg(\mathcal{G}).$$

(ii) If $\dim(\mathcal{E}(\mathcal{I}) \times_A \Bbbk) \leqslant r - 1$*, then*

$$\deg(\mathcal{g}) \geqslant \deg(\mathcal{G}).$$

(iii) Assuming that $\Bbbk$ is algebraically closed, there exists an open dense subset $\mathcal{W} \subset \Bbbk^m$ such that, if $\mathfrak{n} = (z_1 - \alpha_1, \dots, z_m - \alpha_m)$ with $(\alpha_1, \dots, \alpha_m) \in \mathcal{W}$, then we have

$$\deg(\mathcal{g}) \geqslant \deg(\mathcal{G}).$$

(iv) Consider the following condition:
($\mathfrak{K}$) $k \geqslant 0$ is a given integer such that $\ell(\mathcal{I}_\mathfrak{P}) \leqslant \operatorname{ht}(\mathfrak{P}/\mathfrak{n}R) + k$ for every prime ideal $\mathfrak{P} \in \operatorname{Spec}(R)$ containing $(\mathcal{I}, \mathfrak{n})$.

Then:

- *($\mathfrak{K}1$) If ($\mathfrak{K}$) holds with $k \leqslant 1$, then condition (b) of part (i) is satisfied.*
- *($\mathfrak{K}2$) If ($\mathfrak{K}$) holds with $k = 0$, then the assumption of (ii) is satisfied.*

An additional interest in this chapter is the specialization of the saturated fiber cone of $\mathcal{I}$. By letting the specialization be suitably general, we prove that the multiplicity of the saturated special fiber ring of I is equal to the one of the saturated special fiber ring of $\mathcal{I} \otimes_A \operatorname{Quot}(A)$, where $\operatorname{Quot}(A)$ denotes the field of fractions of A. As a consequence, when the coefficients of the forms $\{\overline{g_0}, \ldots, \overline{g_s}\}$ are general, we obtain a formula for the product of the degree of $\mathcal{G}$ and the degree of the image of $\mathcal{G}$.

Let $\mathbb{K} = \operatorname{Quot}(A)$ denote the field of fractions of A and let $\mathbb{T} = \mathbb{K}[x_0, \ldots, x_r]$ denote the standard polynomial ring over $\mathbb{K}$ obtained from $R = A[x_0, \ldots, x_r]$ by base change (i.e., considering the A-coefficients of a polynomial as $\mathbb{K}$-coefficients). In addition, let $\mathbb{G}$ denote the rational map $\mathbb{G} : \mathbb{P}^r_{\mathbb{K}} \dashrightarrow \mathbb{P}^s_{\mathbb{K}}$ defined by the tuple of forms $\{G_0, \ldots, G_s\}$, where G_i is the image of g_i along the canonical inclusion $R \hookrightarrow \mathbb{T}$. Finally, let $Y \subset \mathbb{P}^s_{\Bbbk}$ and $\mathbb{Y} \subset \mathbb{P}^s_{\mathbb{K}}$ be the closures of the images of $\mathcal{G}$ and $\mathbb{G}$, respectively. The following theorem contains the second main result of Chapter 5.

Theorem N (Theorem 5.47)**.** *Suppose that both $\mathcal{G}$ and $\mathcal{G}$ are generically finite. Assuming that $\Bbbk$ is algebraically closed, there exists an open dense subset $\mathcal{V} \subset \Bbbk^m$ such that, if $\mathfrak{n} = (z_1 - \alpha_1, \ldots, z_m - \alpha_m)$ with $(\alpha_1, \ldots, \alpha_m) \in \mathcal{V}$, then we have*

$$\deg(\mathcal{G}) \cdot \deg_{\mathbb{P}^s_{\Bbbk}}(Y) = \deg(\mathbb{G}) \cdot \deg_{\mathbb{P}^s_{\mathbb{K}}}(\mathbb{Y}).$$

As a consequence of Theorem M(iii) and Theorem N we obtain the following corollary.

Corollary O (Corollary 5.48)**.** *Suppose that both $\mathcal{G}$ and $\mathcal{G}$ are generically finite. Assuming that $\Bbbk$ is algebraically closed, there exists an open dense subset $\mathcal{Q} \subset \Bbbk^m$ such that, if $\mathfrak{n} = (z_1 - \alpha_1, \ldots, z_m - \alpha_m)$ with $(\alpha_1, \ldots, \alpha_m) \in \mathcal{Q}$, then we have*

$$\deg_{\mathbb{P}^s_{\Bbbk}}(Y) \leqslant \deg_{\mathbb{P}^s_{\mathbb{K}}}(\mathbb{Y}).$$

The basic outline of Chapter 5 is as follows. In Section 5.1, we fix some terminologies and notations. In Section 5.2, we develop in an algebraic fashion the main points of the theory of rational maps with source and target projective varieties defined over an arbitrary Noetherian integral domain of finite Krull dimension. In Section 5.3, we gather a few algebraic tools to be used in the specialization of rational maps. In Section 5.4, we prove Theorem M, Theorem N and Corollary O. In Section 5.5, we consider the problem of specialization of rational maps in the particular case of perfect base ideals of height two.

III Asymptotic properties of the powers of edge ideals of graphs

Let I be a homogeneous ideal in a polynomial ring $R = \Bbbk[x_1, \ldots, x_r]$ over a field $\Bbbk$. The Castelnuovo-Mumford regularity of I, denoted by $\operatorname{reg}(I)$, has been an interesting and active research topic for the past decades. There exists a vast literature on the study of $\operatorname{reg}(I)$ (see e.g. [25]). A celebrated result on the behavior of the regularity of powers of ideals was proved independently in [42] and [99]. In both papers, by making a detailed study of the Rees algebra of I, it is shown that for all $q \geqslant q_0$, the regularity of the powers of I is asymptotically a linear function $\operatorname{reg}(I^q) = dq + b$,

where q_0 is the so-called stabilizing index, and b is the so-called constant. The value of d in the above formula is well understood (see [139, Theorem 3.2]). For example, d is equal to the degree of the generators of I when I is equigenerated in degree d (see loc. cit.). However, there is no general or precise method to determine q_0 and b.

In recent years, many researchers have tried to compute q_0 and b for special families of ideals. One of the simplest cases, yet interesting and wide open, is when I is the edge ideal of a finite simple graph. Let $G = (V(G), E(G))$ be a finite simple graph on the vertex set $V(G) = \{x_1, \ldots, x_r\}$. The edge ideal $I = I(G)$, associated to G, is the ideal of R generated by the set of monomials $x_i x_j$ such that x_i is adjacent to x_j.

The problem of determining the stabilizing index and the constant have been settled for special families of graphs. The approach is focused on the relations between the combinatorics of graphs and algebraic properties of edge ideals. We refer the reader to see e.g. [3–5, 8–10, 12, 52, 63, 75, 89, 96, 112, 115, 151] for more information on this topic.

In Chapter 6 and Chapter 7, partly inspired by the interest of this problem, we study the regularity of edge ideals and their powers for the families of bipartite graphs and bicyclic graphs, respectively.

Bipartite graphs

In Chapter 6, we consider several aspects of the Rees algebra of the edge ideal of a bipartite graph.

One can find a vast literature on the Rees algebra of edge ideals of bipartite graphs (see e.g. [54, 56, 136, 147–150]), nevertheless, in Chapter 6 we study several properties that might have been overlooked. From a computational point of view we first focus on the universal Gröbner basis of its defining equations, and from a more algebraic standpoint we focus on its total and partial regularities as a bigraded algebra. Applying these ideas, we give an estimation of when $\operatorname{reg}(I^s)$ starts to be a linear function and we find upper bounds for the regularity of the powers of I.

Inside this subsection, let $G = (V(G), E(G))$ be a bipartite graph on the vertex set $V(G) = \{x_1, \ldots, x_r\}$. As before, let $\Bbbk$ be a field, R be the polynomial $R = \Bbbk[x_1, \ldots, x_r]$, and I be the edge ideal $I = I(G)$ of G. Let $f_1, \ldots, f_q$ be the square free monomials of degree two generating I. We can see $\mathcal{R}(I)$ as a quotient of the polynomial ring $S = R[T_1, \ldots, T_q]$ via the map

$$S = \Bbbk[x_1, \ldots, x_r, T_1, \ldots, T_q] \xrightarrow{\Psi} \mathcal{R}(I) \subset R[t], \quad \psi(T_i) = f_i t.$$

Then, the presentation of $\mathcal{R}(I)$ is given by $S/\mathcal{K}$ where $\mathcal{K} = \operatorname{Ker}(\psi)$.

The universal Gröbner basis of the ideal $\mathcal{K}$ is defined as the union of all the reduced Gröbner bases $\mathcal{G}_<$ of the ideal $\mathcal{K}$ as $<$ runs over all possible monomial orders (see [138]). In the first main result of Chapter 6, we compute the universal Gröbner basis of the defining equations $\mathcal{K}$ of the Rees algebra $\mathcal{R}(I)$.

Notation P (Notation 6.3)**.** *Given a walk $w = \{v_0, \dots, v_a\}$, each edge $\{v_{j-1}, v_j\}$ corresponds to a variable T_{i_j}, and we set $T_{w^+} = \prod_{j \text{ is even}} T_{i_j}$ and $T_{w^-} = \prod_{j \text{ is odd}} T_{i_j}$ (in case $a = 1$ we make $T_{w^+} = 1$). We adopt the following notations:*

(i) Let $w = \{v_0, \dots, v_a = v_0\}$ be an even cycle in G. Then, by T_w we denote the binomial

$$T_{w^+} - T_{w^-} \in \mathcal{K}.$$

(ii) Let $w = \{v_0, \dots, v_a\}$ be an even path in G. Then, the path w determines the binomial

$$v_0 T_{w^+} - v_a T_{w^-} \in \mathcal{K}.$$

(iii) Let $w_1 = \{u_0, \dots, u_a\}$, $w_2 = \{v_0, \dots, v_b\}$ be two disjoint odd paths. Let $T_{(w_1,w_2)^+} = T_{w_1^+} T_{w_2^-}$ and $T_{(w_1,w_2)^-} = T_{w_1^-} T_{w_2^+}$, then w_1 and w_2 determine the binomial

$$u_0 u_a T_{(w_1,w_2)^+} - v_0 v_b T_{(w_1,w_2)^-} \in \mathcal{K}.$$

Theorem Q (Theorem 6.5)**.** *Let G be a bipartite graph and $\mathcal{K}$ be the ideal of defining equations of the Rees algebra $\mathcal{R}(I(G))$. The universal Gröbner basis $\mathcal{U}$ of $\mathcal{K}$ is given by*

$$\begin{aligned}\mathcal{U} = &\{T_w \mid w \text{ is an even cycle}\}\\ &\cup \{v_0 T_{w^+} - v_a T_{w^-} \mid w = (v_0, \dots, v_a) \text{ is an even path}\}\\ &\cup \{u_0 u_a T_{(w_1,w_2)^+} - v_0 v_b T_{(w_1,w_2)^-} \mid w_1 = (u_0, \dots, u_a) \text{ and}\\ &\qquad\qquad w_2 = (v_0, \dots, v_b) \text{ are disjoint odd paths}\}.\end{aligned}$$

The polynomial ring S is equipped with the bigrading: $\operatorname{bideg}(x_i) = (1, 0)$ and $\operatorname{bideg}(T_j) = (0, 1)$. The algebra $\mathcal{R}(I)$, as a bigraded S-module, has a minimal bigraded free resolution

$$0 \longrightarrow F_p \longrightarrow \cdots \longrightarrow F_1 \longrightarrow F_0 \longrightarrow \mathcal{R}(I) \longrightarrow 0,$$

where $F_i = \oplus_j S(-a_{ij}, -b_{ij})$. In the same way as in [122], we can define the partial x-regularity of $\mathcal{R}(I)$ by

$$\operatorname{reg}_{\mathbf{x}}(\mathcal{R}(I)) = \max_{i,j}\{a_{ij} - i\},$$

the partial T-regularity by

$$\operatorname{reg}_{\mathbf{T}}(\mathcal{R}(I)) = \max_{i,j}\{b_{ij} - i\},$$

and the total regularity by

$$\operatorname{reg}(\mathcal{R}(I)) = \max_{i,j}\{a_{ij} + b_{ij} - i\}.$$

In the second main result of Chapter 6, we prove that the total regularity of $\mathcal{R}(I(G))$ coincides with the matching number of G and estimate both partial regularities of $\mathcal{R}(I(G))$.

Theorem R (Theorem 6.22)**.** *Let* G *be a bipartite graph. Then, we have:*

(i) $\operatorname{reg}(\mathcal{R}(I(G))) = \operatorname{match}(G)$,

(ii) $\operatorname{reg}_{\mathbf{x}}(\mathcal{R}(I(G))) \leqslant \operatorname{match}(G) - 1$,

(iii) $\operatorname{reg}_{\mathbf{T}}(\mathcal{R}(I(G))) \leqslant \operatorname{match}(G)$,

where $\operatorname{match}(G)$ *denotes the matching number of* G.

In Corollary 6.23, from the Chardin-Römer equality [27, Theorem 3.5], we obtain the upper bound

$$\operatorname{reg}(I(G)^s) \leqslant 2s + \operatorname{reg}_{\mathbf{x}}(\mathcal{R}(I)) \leqslant 2s + \operatorname{match}(G) - 1$$

for any bipartite graph G (this upper bound in some cases is weaker than the one of [90], but it is interesting how it follows from a mostly algebraic method). In Corollary 6.24, by using the relation between the partial T-regularity and the stabilization of the regularity of the powers of I [42, Proposition 3.7], we obtain that

$$\operatorname{reg}(I(G)^{s+1}) = \operatorname{reg}(I(G)^s) + 2.$$

for all $s \geqslant \operatorname{match}(G) + q + 1$.

The basic outline of Chapter 6 is as follows. In Section 6.1, we compute the universal Gröbner basis of $\mathcal{K}$ (Theorem Q). In Section 6.2, we consider a specific monomial order that allows us to get upper bounds for the partial x-regularity of $\mathcal{R}(I)$. In Section 6.3, we exploit the canonical module of $\mathcal{R}(I)$ in order to prove Theorem R. In Section 6.4, we give some general ideas about a conjectured upper bound (Conjecture 6.9).

Bicyclic graphs

In Chapter 7, we study the regularity of the edge ideal and its powers for the case of bicyclic graphs.

A bicyclic graph is a graph containing exactly two cycles. The family of bicyclic graphs has three possible types of base graphs: two cycles joined at a vertex, two cycles connected by a path, and two cycles sharing a path. In [61], it was computed the regularity of all the powers of the edge ideal of a graph given by two cycles joined at a vertex.

In Chapter 7, we consider the family of bicyclic graphs where the base graph is a dumbbell. A dumbbell graph $C_n \cdot P_l \cdot C_m$ is a graph consisting of two cycles C_n and C_m connected with a path P_l, where n, m, and l are the number of vertices. In the example below we show two different dumbbell graphs.

Example S. *Two base cases when* $l = 2$ *and* $l = 1$ *are the following:*

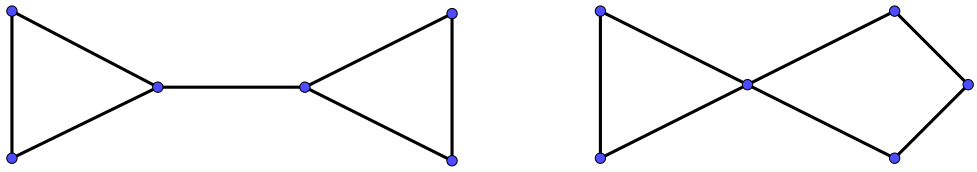

The dumbbell graphs $C_3 \cdot P_2 \cdot C_3$ and $C_3 \cdot P_1 \cdot C_4$.

Notation T. *Let* G *be a graph and* $H \subset G$ *be a subgraph.*

(i) The maximum size of an induced matching in G *is called its induced matching number and it is denoted by* $\nu(G)$.

(ii) $\Gamma_G(H)$ *denotes the subset of vertices*

$$\Gamma_G(H) = \{v \in G \mid d(v, H) = 1\},$$

i.e. the vertices at distance one from H.

(iii) The Lozin transformation of a vertex $x \in G$ *is an operation that replaces* x *by four new vertices, and produces a new graph denoted by* $\mathcal{L}_x(G)$ *(see Definition 7.23).*

From [96, Corollary 1.2] and [11, Theorem 4.11] we have the following inequalities relating $\operatorname{regI}(G)$ and $\nu(G)$ in the case of bicyclic graphs

$$\nu(G) + 1 \leqslant \operatorname{regI}(G) \leqslant \nu(G) + 3.$$

In the main result of Chapter 7, we obtain a full combinatorial characterization of the regularity of the edge ideal of a bicyclic graph G (having a dumbbell subgraph) in terms of the induced matching number of G. This result adds a new family of graphs for which the regularity is known, and extends the results of [4] where the family of unicyclic graphs was studied. For a dumbbell graph $C_n \cdot P_l \cdot C_m$, we always assume that "$n \bmod 3 \leqslant m \bmod 3$". Since the graphs $C_n \cdot P_l \cdot C_m$ and $C_m \cdot P_l \cdot C_n$ are clearly isomorphic, the cases "$n \equiv 2 \pmod 3$, $m \equiv 0, 1 \pmod 3$" have the same results as the cases "$n \equiv 0, 1 \pmod 3$, $m \equiv 2 \pmod 3$".

Theorem U (Theorem 7.64)**.** *Let* G *be a bicyclic graph with dumbbell subgraph* $C_n \cdot P_l \cdot C_m$.

(I) If $n, m \equiv 0, 1 \pmod 3$*, then* $\operatorname{regI}(G) = \nu(G) + 1$.

(II) If $n \equiv 0, 1 \pmod 3$ *and* $m \equiv 2 \pmod 3$*, then*

$$\nu(G) + 1 \leqslant \operatorname{regI}(G) \leqslant \nu(G) + 2,$$

and $\operatorname{regI}(G) = \nu(G) + 2$ *if and only if* $\nu(G) = \nu(G \setminus \Gamma_G(C_m))$.

(III) *If* $n, m \equiv 2 \pmod 3$ *and* $l \geqslant 3$*, then* $\nu(G) + 1 \leqslant \operatorname{regI}(G) \leqslant \nu(G) + 3$*. Moreover:*

(i) $\operatorname{regI}(G) = \nu(G) + 3$ *if and only if* $\nu(G \setminus \Gamma_G(C_n \cup C_m)) = \nu(G)$.

(ii) $\operatorname{regI}(G) = \nu(G) + 1$ *if and only if the following conditions hold:*

(a) $\nu(G) - \nu(G \setminus \Gamma_G(C_n \cup C_m)) > 1$*;*

(b) $\nu(G) > \nu(G \setminus \Gamma_G(C_n))$*;*

(c) $\nu(G) > \nu(G \setminus \Gamma_G(C_m))$.

(IV) *If* $n, m \equiv 2 \pmod 3$ *and* $l \leqslant 2$*, then* $\nu(G) + 1 \leqslant \operatorname{regI}(G) \leqslant \nu(G) + 2$*. Let* x *be a point on the bridge* P_l *and let* $\mathcal{L}_x(G)$ *be the Lozin transformation of* G *with respect to* x *given as in Construction 7.62. Then,* $\operatorname{regI}(G) = \nu(G) + 1$ *if and only if the following conditions are satisfied:*

(a) $\nu(\mathcal{L}_x(G)) - \nu(\mathcal{L}_x(G) \setminus \Gamma_{\mathcal{L}_x(G)}(C_n \cup C_m)) > 1$*;*

(b) $\nu(\mathcal{L}_x(G)) > \nu(\mathcal{L}_x(G) \setminus \Gamma_{\mathcal{L}_x(G)}(C_n))$*;*

(c) $\nu(\mathcal{L}_x(G)) > \nu(\mathcal{L}_x(G) \setminus \Gamma_{\mathcal{L}_x(G)}(C_m))$.

For a particular family of dumbbell graphs, we obtain a formula for the regularity of all the powers of the edge ideal.

Theorem V (Theorem 7.76)**.** *For the dumbbell graph* $C_n \cdot P_l \cdot C_m$ *with* $l \leqslant 2$*, we have*

$$\operatorname{regI}(C_n \cdot P_l \cdot C_m)^q = 2q + \operatorname{regI}(C_n \cdot P_l \cdot C_m) - 2$$

for all $q \geqslant 1$.

The basic outline of Chapter 7 is as follows. In Section 7.1, we recall some preliminary results. In Section 7.2, we compute the induced matching number of a dumbbell graph and the regularity of its edge ideal. In Section 7.3, we prove Theorem U. In Section 7.4, we prove Theorem V.

Note of references

Some parts of this work have already been submitted, published or accepted for publication in:

(1) ([29]) Yairon Cid-Ruiz, *A* D*-module approach on the equations of the Rees algebra*, to appear in J. Commut. Algebra (2017). arXiv:1706.06215.

(2) ([22]) Laurent Busé, Yairon Cid-Ruiz, and Carlos D'Andrea, *Degree and birationality of multigraded rational maps*, ArXiv e-prints (May 2018), available at 1805.05180.

(3) ([30]) Yairon Cid-Ruiz, *Multiplicity of the saturated special fiber ring of height two perfect ideals*, ArXiv e-prints (July 2018). 1807.03189.

(4) ([33]) Yairon Cid-Ruiz and Aron Simis, *Degree of rational maps via specialization*, arXiv preprint arXiv:1901.06599 (2019).

(5) ([31]) Yairon Cid-Ruiz, *Regularity and Gröbner bases of the Rees algebra of edge ideals of bipartite graphs*, Le Matematiche 73 (2018), no. 2, 279–296.

(6) ([32]) Yairon Cid-Ruiz, Sepehr Jafari, Navid Nemati, and Beatrice Picone, *Regularity of bicyclic graphs and their powers*, to appear in J. Algebra Appl. (2018). arXiv:1802.07202.

A *Macaulay2* [60] package that gives support to most of the results of [22] was implemented. This package is capable of computing the saturated special fiber ring (the algebra introduced in [22]) of an ideal in a multi-graded setting. In particular, it provides new algorithms to compute the degree of a rational map and to test birationality. This package is included in the latest versions of *Macaulay2* [60]:

(7) ([28]) Yairon Cid-Ruiz, *MultiGradedRationalMap: Degree and birationality of multi-graded rational maps*. Available at `http://www2.macaulay2.com/Macaulay2/doc/Macaulay2-1.13/share/doc/Macaulay2/MultiGradedRationalMap/html/index.html`.

Chapter 3

Fatmanur Yildirim: Finite fibers of rational maps by means of matrix representations with applications to distance problem

Rational maps are fundamental objects in algebraic geometry. In the field of Computer-Aided Geometric Design (CAGD) and geometric modelling, they are used to describe geometric objects. For instance, the image of rational maps are used to give parametric representations of geometric objects as *parameterisations of for example curves and surfaces*. To illustrate, the unit sphere in $\mathbb{R}^3$ is usually parameterised by the rational map ϕ

$$\begin{array}{rccc} \phi: & \mathbb{A}^2_{\mathbb{R}} & \to & \mathbb{A}^3_{\mathbb{R}} \\ & (u,v) & \mapsto & \left(\frac{2u}{1+u^2+v^2}, \frac{2v}{1+u^2+v^2}, \frac{-1+u^2+v^2}{1+u^2+v^2}\right). \end{array}$$

Parametric algebraic curves and surfaces can be also described by *implicit representations* as the set of points verifying common zeros of polynomial equation(s). To illustrate, we consider again the unit sphere in $\mathbb{R}^3$. Then, the zeros of the equation

$$x^2 + y^2 + z^2 - 1 = 0 \text{ where } (x, y, z) \in \mathbb{R}^3$$

define the unit sphere in $\mathbb{R}^3$, i.e. $x^2 + y^2 + z^2 - 1 = 0$ is its implicit equation. Here, we emphasise that only one polynomial equation is enough to represent implicitly a plane curve, whereas we need several polynomial equations for curves and surfaces in space over $\mathbb{C}$. Both representations are intensively used in Computer-Aided Geometric Design (CAGD) and geometric modelling depending on the problem. Nevertheless, we emphasise that the implicit equation(s) of a given parametric geometric object looses information about parameter values.

Very interesting and useful knowledge about a given geometric object in geometric modelling is how many distinct parameter values correspond to the same point p on the given

object, and what their coordinates are. Indeed, in CAGD, instead of the entire geometric object, generally a patch of it is considered. Equivalently we consider its parameterisation only in some intervals of parameter values. The investigation of which parameter values of p are on the patch requires more information than what the implicit equations provide. Seeking for answers to these questions leads to study the *fibers of the corresponding parameterisation, i.e. rational map.*

Let k be a field and Φ be a rational map from $\mathbb{P}^n_k$ to $\mathbb{P}^m_k$ given by homogeneous polynomials $F_0, \ldots, F_m$ of degree d in the coordinate ring $R = k[x_0, \ldots, x_n]$. Then, the closed image of Φ is a subvariety in $\mathbb{P}^m_k$. Moreover, from the graph Γ_Φ of the rational map Φ, we have two canonical projections, the first one is on the first component, i.e. $\pi_1 : \Gamma_\Phi \to \mathbb{P}^n_k$, the second one is on the last component, i.e. $\pi_2 : \Gamma_\Phi \to \mathbb{P}^m_k$.

$$\begin{array}{ccc} \Gamma_\Phi & \hookrightarrow & \mathbb{P}^n_k \times \mathbb{P}^m_k \\ {\scriptstyle \pi_1}\downarrow & \searrow^{\pi_2} & \\ \mathbb{P}^n_k & \overset{\Phi}{\dashrightarrow} & \mathbb{P}^m_k. \end{array}$$

Then, the closed image of Φ is the image of π_2. We define the *fiber over the point* p in $\mathbb{P}^m_k$ as the pre-images along π_2 of p and we denote it as $\pi_2(p)^{-1}$.

Moreover, the investigation of whether the fiber is empty answers the *implicitisation* problem. *The first part of my thesis studies the fibers of rational maps from $\mathbb{P}^1_k$ to $\mathbb{P}^m_k$, for any integer $m \geqslant 2$ by means of implicit matrices built from both linear (syzygies) and quadratic relations between the coordinates of Φ for the rational algebraic curve implicitisation problem.*

We can describe a rational algebraic surface $\mathcal{S}$ as used in CAGD by a parameterisation of the form $\Phi : X \dashrightarrow \mathbb{P}^3_k$, where X is either $\mathbb{P}^1_k \times \mathbb{P}^1_k$ (rational tensor-product surface) or $\mathbb{P}^2_k$ (rational triangular surface). Let $k[\underline{x}]$ be the coordinate ring of X. We know that in Euclidean geometry the orthogonal projections of a point p onto the surface $\mathcal{S}$ in $\mathbb{P}^3_k$ lie on the normal lines to the surface $\mathcal{S}$ passing through the point p. With the goal to compute the orthogonal projections of p onto $\mathcal{S}$, we study the fiber over p of the *multi-graded dense rational map* Ψ, which is a parameterisation of the normal lines of the surface $\mathcal{S}$. We assume that the fiber over p is finite, i.e. there are finitely many orthogonal projections onto $\mathcal{S}$. The rational map Ψ is of form $\Psi : X \times \mathbb{P}^1_k \to \mathbb{P}^3_k$ such that $\Psi(\underline{x}) = \bar{t}\Phi(\underline{x}) + t\nabla(\underline{x})$, where $\nabla(\underline{x})$ is the homogeneous normal vector to $\mathcal{S}$ and $k[\bar{t}, t]$ is the coordinate ring of the last $\mathbb{P}^1_k$. It is of degree $(\boldsymbol{d}, 1)$ on $X \times \mathbb{P}^1_k$ where $\boldsymbol{d}$ is bidegree if $X = \mathbb{P}^1_k \times \mathbb{P}^1_k$ or $\boldsymbol{d}$ is degree if $X = \mathbb{P}^2_k$. Moreover, for a general rational surface we observe that the base locus of the rational map Ψ, i.e. points in $X \times \mathbb{P}^1_k$ where Ψ_0, Ψ_1, Ψ_2 and Ψ_3 vanish simultaneously is of *dimension one.* Once we know the orthogonal projections of p onto $\mathcal{S}$, then we can compute the distance between the point p and the surface $\mathcal{S}$ which will be the smallest among the distances between p and its orthogonal projections. *In a second part, my thesis studies the finite fibers of multi-graded rational dominant maps onto three dimensional projective space*

and its application to the computation of orthogonal projections of a point onto a rational algebraic surface.

Finally, in the last chapter, my thesis reports on *3-month industrial secondment in Missler Software in France where I treated distance between a circle and a line and also between an arc of a circle and a line segment in space.*

3.1 Curve implicitization

In what follows, we give a short overview about existing works on the implicitisation of plane curves and introduce the contribution of my thesis on this topic. Let $\Phi : \mathbb{P}^1_k \to \mathbb{P}^2_k$ be a parameterization of a plane curve $\mathcal{C}$ given by

$$(s : t) \mapsto (F_0(s,t) : F_1(s,t) : F_2(s,t)),$$

where F_0, F_1, F_2 are homogeneous polynomials of the same degree $d \geqslant 1$ in $k[s,t]$. Implicit representations are particularly interesting for determining whether a point lies on the curve $\mathcal{C}$, also for solving curve/curve intersection problems. Therefore, the implicitisation of rational plane curves have been extensively studied for those reasons in CAGD. One main approach is to use the *resultant*. Let $k[T_0, T_1, T_2]$ be the coordinate ring of $\mathbb{P}^2_k$. Consider the polynomials

$$\begin{aligned} F_0T_1 - F_1T_0 &= a_0(T_0,T_1,T_2)t^d + a_1(T_0,T_1,T_2)st^{d-1} + \cdots + a_d(T_0,T_1,T_2)s^d \quad \text{and} \\ F_0T_2 - F_2T_0 &= b_0(T_0,T_1,T_2)t^d + b_1(T_0,T_1,T_2)st^{d-1} + \cdots + b_d(T_0,T_1,T_2)s^d. \end{aligned}$$

Then, the classical *Sylvester matrix* of $F_0T_1 - F_1T_0$ and $F_0T_2 - F_2T_0$

$$\mathrm{Syl}(F_0T_1 - F_1T_0, F_0T_2 - F_2T_0) = \begin{bmatrix} a_d & & & b_d & & \\ a_{d-1} & \ddots & & b_{d-1} & \ddots & \\ \vdots & \ddots & a_d & \vdots & \ddots & b_d \\ \vdots & & a_{d-1} & \vdots & & b_{d-1} \\ a_0 & & \vdots & b_0 & & \vdots \\ & \ddots & \vdots & & \ddots & \\ & & a_0 & & & b_0 \end{bmatrix}$$

is a $2d \times 2d$ matrix with linear entries in T_0, T_1, T_2 and of which determinant is given by

$$\mathrm{Res}(F_0T_1 - F_1T_0, F_0T_2 - F_2T_0) = T_0^d C(T_0,T_1,T_2)^{\deg(\Phi)},$$

where $C(T_0, T_1, T_2)$ is the implicit equation of the curve (defined up to a nonzero constant factor) and $\deg(\Phi)$ is the degree of the map Φ. When k is algebraically closed, then $\deg(\Phi)$ is the number of pre-images of a generic point on the curve $\mathcal{C}$ via Φ.

There exist also the methods based on *moving lines* for the implicitisation problem. The moving lines have been introduced by Sederberg and Chen in [5]. A moving line L is a polynomial

$$L(T_0, T_1, T_2; s, t) := A(s,t)T_0 + B(s,t)T_1 + C(s,t)T_2.$$

For fixed s, t values, the equation $L = 0$ defines a line that moves when the parameter value s, t of the curve moves. We say that the moving line L follows the rational plane curve $\mathcal{C}$ if

$$L(\Phi(s,t); s, t) = A(s,t)F_0(s,t) + B(s,t)F_1(s,t) + C(s,t)F_2(s,t) = 0.$$

Let $I := (F_0, F_1, F_2)$ be the ideal of $k[s,t]$. *The syzygy module of the ideal* I is defined as

$$\mathrm{Syz}(I) := \{(g_0, g_1, g_2) \in k[s,t]^3 : g_0F_0 + g_1F_1 + g_2F_2 = 0\}.$$

Thus, $(A(s,t), B(s,t), C(s,t))$ is a syzygy of I if L follows Φ. Moreover it is known that $\mathrm{Syz}(F_0, F_1, F_2)$ is a free $k[s,t]$-module of rank 2 (see [6]). We denote a couple of generators by $p := (p_0, p_1, p_2)$ and $q := (q_0, q_1, q_2)$. The couple p, q is called a *μ-basis* (see [6]). Let $\deg(p) = \mu_1, \deg(q) = \mu_2$ and $\mu_1 \leqslant \mu_2$. The μ-basis p, q verifies $\mu_1 + \mu_2 = d$. It is known that for a general plane curve of degree d, we have $\mu_2 = \left\lceil \frac{d}{2} \right\rceil$ (see [7]).

There are several existing works on μ-basis. In [7], the method of moving lines following a given plane curve is studied with μ-basis notion. Later in [8], more properties and equivalent definitions of a μ-basis of I for a rational plane curve are given in terms of moving line method with an algorithm based on Gaussian elimination computing the μ-basis. In [5], matrix of moving lines is interpreted as the Sylvester matrix of μ-basis of I, denoted by $\mathrm{Syl}(p, q)$. $\mathrm{Syl}(p, q)$ is of size $d \times d$ of which determinant yields a polynomial of degree d in $k[T_0, T_1, T_2]$. We remark that the matrix $\mathrm{Syl}(p, q)$ has half size of the matrix $\mathrm{Syl}(F_0T_1 - F_1T_0, F_0T_2 - F_2T_0)$, which implies that the use of μ-basis allows us to decrease the size of the implicit matrix whose determinant yields the implicit equation of $\mathcal{C}$. Moreover, the matrix $\mathrm{Syl}(p, q)$, without computing its determinant, can be used for determining if a point lies on the curve simply by evaluating its rank at this point. Then its parameter(s) can be determined from the kernel of this matrix, whereas this is not possible to do with an implicit polynomial equation of the curve $\mathcal{C}$. For that reason, *instead of dealing with the polynomials of higher degree obtained by such determinants, the developed results in my thesis focus on the matrix itself as an implicit representation of the curve* $\mathcal{C}$.

In Chapter 2 of my thesis, we consider Hybrid Bézout matrices of μ-basis that we denoted by $\mathbb{MQ}$. Let p and q be as follows,

$$p = a_0(T_0, T_1, T_2)t^{\mu_1} + a_1(T_0, T_1, T_2)st^{\mu_1 - 1} + \cdots + a_{\mu_1}(T_0, T_1, T_2)s^{\mu_1},$$

$$q = b_0(T_0, T_1, T_2)t^{\mu_2} + b_1(T_0, T_1, T_2)st^{\mu_2 - 1} + \cdots + b_{\mu_2}(T_0, T_1, T_2)s^{\mu_2}.$$

For plane curves, $\mathbb{MQ}$ is $\mu_2 \times \mu_2$ matrix which is composed by the last $\mu_2 - \mu_1$ columns of $\mathrm{Syl}(p, q)$ in coefficients of q and the first μ_1 columns of Bézout matrix of p and q. We recall

that the Bézout matrix of p, q, denoted by $\mathrm{Bez}(p,q)$ is defined by $\mathrm{Bez}(p,q) = (b_{ij})_{1\leqslant i,j\leqslant d}$ where

$$\frac{p(\sigma,\tau)q(s,t) - p(s,t)q(\sigma,\tau)}{s\tau - t\sigma} = \sum_{1\leqslant i,j\leqslant d} b_{ij} t^{i-1} s^{d-i+1} \tau^{j-1} \sigma^{d-j+1},$$

and σ, τ are new indeterminates. Since $\mathrm{Bez}(p,q)$ has quadratic entries in T_0, T_1, T_2, Hybrid Bézout matrix consists of both linear and quadratic terms and its determinant yields a homogeneous polynomial of degree $(\mu_2 - \mu_1) + 2\mu_1 = d$ in T_0, T_1, T_2. This approach for obtaining such more compact implicitisation matrices with some quadratic entries is also known as the method of moving conics (see [9]). A *moving conic* of degree ν in $\mathbb{N}$ is a polynomial of the form

$$\begin{aligned} Q(s,t;T_0,T_1,T_2) = g_{0,0}(s,t)T_0^2 + g_{0,1}(s,t)T_0T_1 + \\ g_{0,2}(s,t)T_0T_2 + g_{1,1}(s,t)T_1^2 + g_{1,2}(s,t)T_1T_2 + g_{2,2}(s,t)T_2^2 \end{aligned}$$

where the polynomials $g_{i,j}(s,t)$ are homogeneous polynomials of degree ν in $k[s,t]$. In addition, this moving conic is said to follow the parameterisation ϕ if

$$Q(s,t;F_0,F_1,F_2) = \sum_{0\leqslant i\leqslant j\leqslant 2} g_{i,j}(s,t)F_i(s,t)F_j(s,t) = 0.$$

Similarly to moving lines, this latter condition means geometrically that the conic Q goes through the point $\phi(s:t) \in \mathcal{C}$. The moving conics have been introduced in [10] and then extensively used, especially to deal with the implicitisation of rational surfaces (see [11, 9]).

Unlike the case of plane curves, the implicitisation of parameterised curves in higher dimension is much more delicate because now a space curve is not given by a single equation over algebraically closed field. Nevertheless, the concept of μ-basis is easily generalized to curves in higher dimension [12, 13] and many results to produce some implicit polynomial equations of a curve from them have been proposed. For instance [14] and [15] consist in using the elimination matrix built from a μ-basis as an implicit representation. Thus, this matrix of moving hyperplanes denoted by $\mathbb{M}$ is the natural generalisation of the Sylvester matrix of a μ-basis in the case of plane curves. Although this matrix is no longer a square matrix, it still allows to characterise the point that lie on the curve by a drop of its rank. In [14], the construction and the properties of the matrix of moving hyperplanes $\mathbb{M}_\nu$ has been studied. Briefly, the matrix $\mathbb{M}_\nu$ is filled by the syzygies of the ideal generated by the coordinates of a parameterisation of the space curve of a suitable degree ν. We will say that $\mathbb{M}_\nu$ is the matrix of moving hyperplanes at given degree ν. Some applications such that inversion of a point on a curve by means of generalised eigenvalues computation, multiplicity of a point p on a curve by means of drop of rank of $\mathbb{M}_\nu$ evaluated at p are explained in details. Furthermore, intersection problems are studied. More precisely, intersection of two curves is studied by substituting the parameterisation of the first curve $\mathcal{C}_1$ into a suitable implicit matrix $\mathbb{M}_\nu$ of the second curve $\mathcal{C}_2$. Then, one may consider the two companion matrices of

the cokernel of $\mathbb{M}_2$, then reduce them into two square full rank matrices by Kronecker form (see [16, §3.2], [14, §6.2.]), and after that compute their generalised eigenvalues in order to compute the coordinates of the intersection points. Similar matrices are also used for curve/surface, surface/surface intersection problems (see [17, 16]).

From now on, let Φ be the parameterisation

$$\begin{array}{rccc} \Phi: & \mathbb{P}^1_k & \to & \mathbb{P}^m_k \\ & (s:t) & \mapsto & (F_0(s,t):F_1(s,t):\ldots:F_m(s,t)) \end{array}$$

where $F_0,\ldots,F_m$ are homogeneous polynomials of degree $d \geqslant 1$ in $k[s,t]$. Let $I := (F_0,\ldots,F_m)$ be an ideal of $k[s,t]$. Then, the μ-basis notion can be generalised to higher dimensions $m \geqslant 2$ for curves, since the syzygy module of I, denoted by $\mathrm{Syz}(I)$, is still free and $\mathrm{Syz}(I)$ is generated by m vectors of homogeneous polynomials, whose degrees sum up to d, according to Hilbert-Burch Theorem (see [18]). We will still assume that $\mu_1 \leqslant \cdots \leqslant \mu_m$, where μ_i's are the degrees of μ-basis. We refer the reader to the work [13] which generalises moving line methods in [8] into higher dimensions, i.e. generalises to the rational space curves in arbitrary dimension. In addition, [19] gives explicitly the properties of μ-basis of space curve parameterisation Φ with an algorithm based on partial reduced row-echelon form of a coefficient matrix of Sylvester type which is faster than the previous known methods in [13, 8].

Back to the use of resultant type matrices for implicitisation problem, in Chapter 2 of my thesis we generalise the Hybrid Bézout matrix of μ-basis into higher dimensions. We construct it by concatenating the matrix of moving hyperplanes and matrix of moving quadrics at given degree ν and denote it by $\mathbb{MQ}$. We also show the strong relation between the matrices $\mathbb{MQ}$ and degree of the fiber over a point p on the given curve $\mathcal{C}$.

We first recall that for all R-module M where R is a graded ring and $k = R_0$ is a field, we define *Hilbert function of* M as

$$HF_M(\mu) = \dim_k(M_\mu),$$

and *Hilbert series of* M as

$$HS_M(x) = \sum_{\mu\in\mathbb{Z}} \dim_k(M_\mu)x^\mu = \frac{L_M(x)}{(1-x)^\delta},$$

where δ denotes the Krull dimension of M and $L_M(x)$ is the unique polynomial verifying $L_M(a) \neq 0$ (see [20, §1.9], [18, Chapter 4]). We define *Hilbert polynomial of* M as

$$HP_M(\mu) = \frac{a_{\delta-1}}{(\delta-1)!}x^{\delta-1} + \cdots + a_0,$$

where $a_{\delta-1} = L_M(1)$. We also know that for all sufficiently large μ, Hilbert function is equal to Hilbert polynomial. Let p be a point in $\mathbb{P}^m_k$ having finite fiber $\pi_2^{-1}(p)$. Then, for the μ

degrees where the Hilbert function of $\pi_2^{-1}(p)$ is equal to the Hilbert polynomial of $\pi_2^{-1}(p)$, it is also equal to the degree of $\pi_2^{-1}(p)$.

Main result 1. Assume that $\nu \geqslant \mu_m - 1$. Let r_ν be the dimension of the vector space of moving hyperplanes in degree ν. Let c_ν be the dimension of the quotient vector space obtained as the vector space of moving quadrics modulo the vector space of moving hyperplanes, both in degree ν. Then, $r_\nu + c_\nu \geqslant \nu + 1$ and the degree of the fiber at $p \in \mathcal{C}$ is equal to corank of $\mathbb{MQ}_\nu(p)$. In particular,

$$\operatorname{rank}(\mathbb{MQ}_\nu(p)) < \nu + 1 \iff p \in \mathcal{C}.$$

Moreover, we have that

$$c_\nu = \sum_{1 \leqslant i < j \leqslant m} \max(0, \mu_i + \mu_j - 1 - \nu).$$

Also, if $\nu \geqslant \mu_m + \mu_{m-1} - 1$ then $c_\nu = 0$ and it follows that $\mathbb{MQ}_\nu = \mathbb{M}_\nu$.

After that, the structure of Hybrid Bézout is explained. Its quadratic relations are computed by Sylvester forms of μ-basis $p_1, \ldots, p_m$ of the parameterisation Φ. Let's first define *Sylvester forms*. Let $k[T_0, \ldots, T_m]$ be the coordinate ring of $\mathbb{P}_k^m$. Let $\mu_i \leqslant \mu_j$ be degrees of p_i and p_j. Let $\alpha := (\alpha_i, \alpha_j)$ be any couple of non-negative integers such that $|\alpha| := \alpha_i + \alpha_j \leqslant \mu_i - 1$. Since p_i and p_j are homogeneous polynomials in the variables s, t, one can decompose them as

$$\begin{aligned} p_i &= s^{\alpha_i+1} h_{i,1} + t^{\alpha_j+1} h_{i,2}, \\ p_j &= s^{\alpha_i+1} h_{j,1} + t^{\alpha_j+1} h_{j,2}, \end{aligned}$$

where $h_{k,h}(s, t; T_0, \ldots, T_m)$ are homogeneous polynomials of degree $\mu_k - \alpha_h - 1$ with respect to the variables s, t and linear forms with respect to the variables $T_0, \ldots, T_m$. Then, we define the polynomial

$$\operatorname{syl}_\alpha(p_i, p_j) := \det \begin{pmatrix} h_{i,1} & h_{i,2} \\ h_{j,1} & h_{j,2} \end{pmatrix}$$

and call it a *Sylvester form* of p_i and p_j. Then, for any integer ν consider the vector space S_ν that is generated by all the Sylvester forms of degree ν, i.e.

$$\mathrm{S}_\nu = \langle \operatorname{syl}_\alpha(p_i, p_j) \text{ such that } \ 1 \leq i < j \leq m \text{ and } |\alpha| = \mu_i + \mu_j - 2 - \nu \rangle .$$

Main result 2. If $\nu \geq \mu_m - 1$, then the moving quadrics of degree ν following Φ are generated by the moving hyperplanes of degree ν following Φ and by the Sylvester forms of degree ν. Moreover, these latter Sylvester forms are linearly independent and hence

$$\dim(\mathrm{S}_\nu) = c_\nu = \sum_{1 \leqslant i < j \leqslant m} \max(0, \mu_i + \mu_j - \nu - 1).$$

3.2 Fibers of rational maps in dimension three

In what follows, a new method to study fibers of multi-graded rational dominant maps onto three dimensional space is presented. We start by mentioning some related works on fibers of rational maps emphasising their assumptions on base locus before explaining our results that are described in Chapter 3 of my thesis.

There exist many related works on properties of rational maps for instance their degrees (see [21, 22, 23, 24]), dimensions, and Jacobian matrices (see [25, 26]), birationality criteria (see [27, 26]), also on equations of Rees algebra of the ideal generated by the coordinates of the rational maps ([28, 29, 30, 31, 32]). We notice that mostly all these works assume that the base locus of the rational map is either empty or zero-dimensional (consists of finite number of isolated points).

In [33], degree and dimension of the fibers of a birational map $\Phi : X \dashrightarrow \mathbb{P}^3_k$ where X is either $\mathbb{P}^2_k$ or $\mathbb{P}^1_k \times \mathbb{P}^1_k$ (or more generally a toric variety), under assumption that *the base locus $\mathcal{B}$ of the rational map Φ consists of finitely many points and $\mathcal{B}$ is locally a complete intersection*, are studied in terms of singular matrices $\mathbb{M}$ based on some syzygies of Φ. The degree of the fiber over the point p in $\mathbb{P}^3_k$ is given in terms of corank of $\mathbb{M}$ evaluated at p.

In [25], the fibers of rational maps $\Phi : \mathbb{P}^n_k \dashrightarrow \mathbb{P}^m_k$ where Φ is generically finite onto its image are studied. It is shown that the number of $(n-1)$-dimensional fibers of such rational map Φ is bounded linearly in terms of the degree of the polynomials defining Φ. The result is obtained by studying the ideals of minors of the Jacobian matrix of Φ. In this approach, Φ is assumed to have *(possibly empty) base locus $\mathcal{B}$ containing finitely many points, which is not necessarily locally a complete intersection.* Moreover, Φ is assumed to be generically finite onto its image.

Later in [34], the multi-graded rational maps $\Phi : \prod_{1\leqslant i\leqslant s} \mathbb{P}^{r_i}_k \dashrightarrow \mathbb{P}^m_k$ with $m = 1 + \sum_{1\leqslant i\leqslant s} r_i$ and *finite base locus* are studied for the implicitisation of rational multiprojective hypersurfaces.

As far as we know the rational maps having *base locus of dimension one* were treated for the first and only time in [35] for the problem of hypersurface implicitisation, i.e. for computing the equation of the closed image of for instance the map $\Phi : \mathbb{P}^{m-1}_k \dashrightarrow \mathbb{P}^m_k$.

In Chapter 3, we study the finite fibers of multi-graded, dense, rational maps $\Psi : X \times \mathbb{P}^1_k \dashrightarrow \mathbb{P}^3_k$, where X is either $\mathbb{P}^1_k \times \mathbb{P}^1_k$ or $\mathbb{P}^2_k$. Such a map Ψ is defined by the homogeneous polynomials $\Psi_0, \Psi_1, \Psi_2, \Psi_3$ of the same degree $(\boldsymbol{d}, e)$ over homogeneous coordinate ring $R := k[\underline{x}, t, \bar{t}] = k[\underline{x}] \otimes_k k[t, \bar{t}] = R_X \otimes R_1$ with k is a field and $\underline{x} = (x_0, \ldots)$, $R_X = k[\underline{x}]$ and $R_1 = k[t, \bar{t}]$ are the coordinate ring of X and $\mathbb{P}^1_k$ respectively. Hence, $(\boldsymbol{d}, e)$ is the degree on $X \times \mathbb{P}^1_k$. The main difficulty that we dealt with in Chapter 3 of the thesis is coming from our assumption that Ψ has a *one dimensional base locus $\mathcal{B}$*, i.e. the variety on which the coordinates of Ψ vanish has at most one-dimensional component. This latter requirement is the most technical property that is treated in my thesis.

Our contribution is more general. More precisely we consider any such rational map Ψ of degree $(\boldsymbol{d}, e)$ from $X \times \mathbb{P}^1_k$ to $\mathbb{P}^3_k$. Since the fibers of the rational map Ψ are not well defined, we need to consider its graph. The defining equations of this graph are known to be the equations of the multi-graded Rees algebra of the ideal I generated by the coordinates of Ψ, that we denote by $\mathrm{Rees}(I)$.

We recall that *Rees algebra* of the ideal $I := (\Psi_0, \Psi_1, \Psi_2, \Psi_3)$ with respect to the ring R is

$$\mathrm{Rees}(I) := \oplus_{i \geqslant 0} I^i z^i \subset R[z].$$

The Rees algebra $\mathrm{Rees}(I)$ inherits the multi-grading via the natural map

$$\begin{array}{rccc} \alpha: & R[T_0, T_1, T_2, T_3] & \to & \mathrm{Rees}(I) \subset R[z] \\ & T_i & \mapsto & \Psi_i z. \end{array}$$

It is known that it is difficult to compute the equations of Rees algebra, for this reason we approximate Rees algebra by symmetric algebra. We refer the reader to [36, 37, 38] for further details about Rees algebra.

Let's denote the ring $R[T_0, T_1, T_2, T_3]$ by S and the ring $k[T_0, T_1, T_2, T_3]$ by R'. Let $\ker(\alpha) = \mathfrak{p}$ an homogeneous ideal of S. We set $\mathfrak{p}_{(\boldsymbol{\mu},\nu)} \subset R_{\boldsymbol{\mu}} \otimes_k R'_\nu$, namely $\boldsymbol{\mu}$ is degree over $X \times \mathbb{P}^1_k$ and ν is degree over $\mathbb{P}^3_k$. We have the S-ideal generated by the syzygies of the ideal $I := (\Psi_0, \ldots, \Psi_3)$, i.e.

$$(\mathfrak{p}_{(*,1)}) = \left(\sum_{i=0}^{3} g_i T_i : g_i \in R \text{ and } \sum_{i=0}^{3} g_i \Psi_i = 0 \right).$$

Moreover, we have the following surjective maps

$$S \to S/(\mathfrak{p}_{(*,1)}) \simeq \mathrm{Sym}(I) \text{ and } \mathrm{Sym}(I) \to \mathrm{Rees}(I) \simeq S/(\mathfrak{p}),$$

where $\mathrm{Sym}(I)$ is called the *symmetric algebra* of the ideal I. Consider the graph Γ_Ψ of Ψ:

$$\begin{array}{ccc} \Gamma_\Psi & \hookrightarrow & X \times \mathbb{P}^3_k \\ {\scriptstyle \pi_1}\downarrow & \swarrow_{\pi_2} & \\ X & \overset{\Phi}{- - \to} & \mathbb{P}^3_k \end{array}$$

We define the fiber over the point $p \in \mathbb{P}^3_k$ as the pre-images along π_2 of p, i.e. $\pi_2(p)^{-1}$. In particular, the fiber over p is a subscheme $\mathfrak{F}_p = \mathrm{Proj}(\mathrm{Rees}(I) \otimes \kappa(p)) \subset X \times \mathbb{P}^1_k$, where $\kappa(p)$ is the residue field of p. We consider symmetric algebra of the ideal I, more precisely the subscheme $\mathfrak{L}_p = \mathrm{Proj}(\mathrm{Sym}(I) \otimes \kappa(p))$ of $X \times \mathbb{P}^1_k$. We call $\mathfrak{L}_p$ as the *linear fiber of* p. We notice that the fiber $\mathfrak{F}_p$ is always contained in the linear fiber $\mathfrak{L}_p$.

For both $X = \mathbb{P}^1_k \times \mathbb{P}^1_k$ and $X = \mathbb{P}^2_k$, we give threshold degrees depending of the degree $(\boldsymbol{d}, e)$ of the Ψ_i's. Beyond these threshold degrees, let's denote them as $(\boldsymbol{\mu}, \nu)$, Hilbert

function of the linear fiber at p evaluated at $(\boldsymbol{\mu}, \nu)$, denoted by $HF_{\mathrm{Sym}(I)\otimes\kappa(p)}(\boldsymbol{\mu}, \nu)$ is equal to Hilbert polynomial of the linear fiber at p evaluated at $(\boldsymbol{\mu}, \nu)$, denoted by $HP_{\mathrm{Sym}(I)\otimes\kappa(p)}(\boldsymbol{\mu}, \nu)$. In the case where the fiber π_2^{-1} is finite, $HP_{\mathrm{Sym}(I)\otimes\kappa(p)}(\boldsymbol{\mu}, \nu)$ is nothing but the degree of the linear fiber at p, which implies it is the number of the orthogonal projections of p onto the given surface. For this reason, we study the vanishings of the local cohomology modules of the linear fiber over the irrelevant ideal $B = (\underline{x}) \cdot (t, \bar{t})$ of the ring R. Moreover, we fill a matrix with syzygies of I at degree beyond the threshold degree. We denote this matrix as $\mathbb{M}_{(\boldsymbol{\mu},\nu)}(\Psi)$. Then, for any point $p \in \mathbb{P}_k^3$ the corank of the matrix evaluated at p, denoted as $\mathbb{M}_{(\boldsymbol{\mu},\nu)}(p)$, is equal to the Hilbert function of the linear fiber at p in degree $(\boldsymbol{\mu}, \nu)$.

Similar to the work [39], the study of linear fiber of the rational map Ψ defined as before requires some assumptions on dimension one components of the base locus $\mathcal{B}$ of Ψ. For this purpose, we introduce the following definition.

Definition. A curve $\mathcal{C} \subset X \times \mathbb{P}_k^1$ is said to have *no section in degree* $< (\boldsymbol{a}, b)$ if $H^0(\mathcal{C}, \mathcal{O}_{\mathcal{C}}(\boldsymbol{\alpha}, \beta)) = 0$ for any degree $(\boldsymbol{\alpha}, \beta)$ such that $\boldsymbol{\alpha} < \boldsymbol{a}$ and $\beta < b$, i.e. if $\mathcal{C}$ has no global section in degree $< (\boldsymbol{a}, b)$.

Lastly before giving our main results, for simplicity we introduce a notation :

Notation. Let r be a positive integer. For any $\boldsymbol{\alpha} = (\alpha_1, \ldots, \alpha_r) \in (\mathbb{Z} \cup \{-\infty\})^r$ we set

$$\mathbb{E}(\boldsymbol{\alpha}) := \{\boldsymbol{\zeta} \in \mathbb{Z}^r \mid \zeta_i \geqslant \alpha_i \text{ for all } i = 1, \ldots, r\}.$$

It follows that for any $\boldsymbol{\alpha}$ and $\boldsymbol{\beta}$ in $(\mathbb{Z} \cup \{-\infty\})^r$ we have that $\mathbb{E}(\boldsymbol{\alpha}) \cap \mathbb{E}(\boldsymbol{\beta}) = \mathbb{E}(\boldsymbol{\gamma})$ where $\gamma_i = \max\{\alpha_i, \beta_i\}$ for all $i = 1, \ldots, r$, i.e. $\boldsymbol{\gamma}$ is the maximum of $\boldsymbol{\alpha}$ and $\boldsymbol{\beta}$ component-wisely.

Main result 3. Assume that we are in one of the two following cases:

(a) The base locus $\mathcal{B}$ is finite, possibly empty,

(b) $\dim(\mathcal{B}) = 1$, the top unmixed one-dimensional curve component $\mathcal{C}$ of $\mathcal{B}$ has no section in degree $< (\mathbf{0}, e)$ and $I^{\mathrm{sat}} = I'^{\mathrm{sat}}$ where I' is an ideal generated by three general linear combinations of the polynomials $\Psi_0, \ldots, \Psi_3$.

Let p be a point in $\mathbb{P}_k^3$ such that $\mathfrak{L}_p$ is finite, then

$$\operatorname{corank} \mathbb{M}_{(\boldsymbol{\mu},\nu)}(p) = \deg(\mathfrak{L}_p)$$

for any degree $(\boldsymbol{\mu}, \nu)$ such that

- if $X = \mathbb{P}_k^2$,
$$(\boldsymbol{\mu}, \nu) \in \mathbb{E}(3d - 2, e - 1) \cup \mathbb{E}(2d - 2, 3e - 1).$$
- if $X = \mathbb{P}_k^1 \times \mathbb{P}_k^1$,
$$(\boldsymbol{\mu}, \nu) \in \mathbb{E}(3d_1 - 1, 2d_2 - 1, e - 1) \cup \mathbb{E}(2d_1 - 1, 3d_2 - 1, e - 1) \cup \mathbb{E}(2d_1 - 1, 2d_2 - 1, 3e - 1).$$

Our motivation to study the fibers of multi-graded rational map Ψ is to compute the orthogonal projections of a point in $\mathbb{P}^3_k$ onto a given surface. However, the hypothesis $I^{\text{sat}} = I'^{\text{sat}}$ where I' is an ideal generated by three general linear combinations of the polynomials $\Psi_0, \ldots, \Psi_3$ is rarely fulfilled, particularly if Ψ is a parameterisation of the congruence of normal lines to a given surface. For that reason, we use explicitly the fact that the base locus $\mathcal{B}$ of Ψ has a known dimension one component in order to compute the degree of linear fiber. Let's denote the top unmixed one-dimensional curve component of $\mathcal{B}$ by $\mathcal{C}$.

Main result 4. Assume that $\dim(\mathcal{B}) = 1$ and that $\mathcal{C}$ has no section in degree $< (\mathbf{0}, e)$. Moreover, assume that there exists an homogeneous ideal $J \subset R$ generated by a regular sequence (g_1, g_2) such that $I \subset J$ and $(I : J)$ defines a finite subscheme in $X \times \mathbb{P}^1_k$. Denote by $(\boldsymbol{m}_1, n_1)$, resp. $(\boldsymbol{m}_2, n_2)$, the degree of g_1, resp. g_2. If $X = \mathbb{P}^2_k$ then $\boldsymbol{m_1}, \boldsymbol{m_2}$ are degrees, if $X = \mathbb{P}^1_k \times \mathbb{P}^1_k$ then $\boldsymbol{m_1}, \boldsymbol{m_2}$ are bidegrees such that $\boldsymbol{m_1} = (m_{1,1}, m_{1,2})$ and $\boldsymbol{m_2} = (m_{2,1}, m_{2,2})$. Set $\eta := \max(e - n_1 - n_2, 0)$ and let p be a point in $\mathbb{P}^3_k$ such that $\mathfrak{L}_p$ is finite. Then,

$$\operatorname{corank} \mathbb{M}_{(\boldsymbol{\mu},\nu)}(p) = \deg(\mathfrak{L}_p)$$

for any degree $(\boldsymbol{\mu}, \nu)$ such that

(a) if $X = \mathbb{P}^2_k$

$$(\mu, \nu) \in \mathbb{E}(3d - 2, e - 1 + \eta) \cup \mathbb{E}(3d - 2 - \min\{\boldsymbol{m_1}, \boldsymbol{m_2}\}, 3e - 1).$$

(b) if $X = \mathbb{P}^1_k \times \mathbb{P}^1_k$

$$\begin{aligned}(\boldsymbol{\mu}, \nu) \in \mathbb{E}(3d_1 - 1, 2d_2 - 1 + \tau_2, e - 1 + \eta) \cup \\ \mathbb{E}(2d_1 - 1 + \tau_1, 3d_2 - 1, e - 1 + \eta) \cup \\ \mathbb{E}(2d_1 - 1 + \tau_1, 2d_2 - 1 + \tau_2, 3e - 1), 1\end{aligned}$$

where $\tau_i := d_i - \min\{2m_{1,i} + m_{2,i}, m_{i,1} + 2m_{2,i}, d_i\} \geqslant 0,\ i = 1, 2.$

In the same chapter of the thesis, the computation of $\mathbb{M}_{(\boldsymbol{\mu},\nu)}(\Psi)$ is described as a null space of a linear system, and corresponding MACAULAY2 code is also given with. We emphasise that the matrix $\mathbb{M}_{(\boldsymbol{\mu},\nu)}(\Psi)$ does not depend on the chosen point p in $\mathbb{P}^3_k$. Namely, once we compute it, we store and use it for any p in $\mathbb{P}^3_k$. After computing the matrix $\mathbb{M}_{(\boldsymbol{\mu},\nu)}(\Psi)$, for any point p in $\mathbb{P}^3_k$ having finite fiber, we describe how to compute the coordinates of the orthogonal projections of p onto the given surface by using generalised eigenvalues and eigenvectors computations. Even if we introduce a new algebraic method, it allows the use of numerical approximations, i.e. floating-point data relying on numerical linear algebra. Lastly, we observe that the computations over the rational field takes much more time than the computations on floating points, since the coefficients gets bigger along the calculations. For that reason, we give a bound for the height of the matrix $\mathbb{M}_{(\boldsymbol{\mu},\nu)}(\Psi)$, in terms of the height of Ψ with respect to p-adic and absolute valuation, degree of the polynomials which define the parameterisation of the given surface and the degree $(\boldsymbol{\mu}, \nu)$.

Three-month industrial secondment at Missler Software

Appendix A of the thesis consists of the technical report which explains two distance problems in space which I treated during my 3-month secondment in Missler Software in Toulouse in France based on some methods in symbolic computation. The aim of my stay was only to transfer some known algebraic approaches for solving the following problems. Problem 1 is the distance between a circle and a line in 3D and Problem 2 is the distance between an arc of a circle and a segment of line in three dimensional space. These problems were chosen to improve some existing algorithms in terms of accuracy and the time computation. Since, after all experiments we have seen that the new algorithms are faster and they get more accurate solutions, I have integrated the algorithms into the interface of TopSolid. They are going to be used in the next version of TopSolid.

Firstly, two implemented algorithms in the CAD Software TopSolid (in programming language C#) to compute the distance between a circle and a line in space are described briefly. One of the algorithms depends on the parameter value of the circle and the other one depends on the parameter value of the line.

After that, my new algorithm for the distance between a line and a circle is explained. The algorithm handles the problem in three different cases : the line is perpendicular to the plane where the circle is located, the line is in the same plane as the circle, and the other situations. First two cases use the elementary Euclidean geometry, and the third case studies the resultant of two partial derivatives of the distance function between a circle and a line. This particular problem of distance yields a resultant which is a univariate polynomial of degree four. I had two main reasons to split the algorithm into several cases. First, the elementary geometry is enough for first two cases, and second the computation time for them using elementary geometry is faster. Then in the section, the number of the real solutions of such a resultant is studied by a root classification of a polynomial of degree four.

Then, my new algorithm for the distance between an arc of a circle and a line segment is described. This algorithm is based on each critical points of the distance between the circle containing the given arc and the line containing the given line segment, which are the extremities of the arc and the segment with the parameter values that are obtained by the resultant.

Lastly, the computational observations such as tolerance choice at several steps in the algorithms are explained. The comparisons between existing algorithms and the algorithms that I implemented are described with some examples.

Chapter 4

Alvaro Fuentes: Modelling shapes with skeletons: scaffolds and anisotropic convolution

This introductory chapter provides an overview of the contributions in the author's PhD thesis. Since we kept the chapters of the thesis as close as possible to their original publications, more discussion on the state of the art can be found within the individual chapters.

Modeling shapes with skeletons has proved useful in many applications, as discussed in the very good survey in [40]. A skeleton, made of a set of curves and/or surfaces centered inside a shape, provides a structure that encapsulates some properties of the shape while also being easier to manipulate. In this work we focus on two geometric modeling applications for 1D skeletons: the generation of a surrounding mesh and the construction of an implicit surface. There is special emphasis on the mathematical foundations of the constructions we propose.

Scaffolds. Generally speaking a *scaffold* is a mesh constructed around a skeleton made of line segments and such that it "follows" the skeleton (see chapters 1 and 2 of the thesis. A simple way to look at a scaffold is as a "thickening" of a 1D skeleton into a surface (see Figure 4.1). One can also say that a scaffold is a "cage-like" or "truss" structure.

These structures are key steps in many applications. They have been used for artistic purposes [41, 42], in architecture [43], for modeling [44, 45], sculpting modeling [46, 47], compatible quadrangulation [48], semi-regular quad meshing [49], volumetric hexahedral meshing [50], cage generation for posing [51], and others.

For most applications, quad-dominant scaffolds are desirable, that is scaffolds with a majority of quad patches. The main difficulties in the generation of scaffolds arise from the presence of cycles and high valency *joints* (nodes where several skeleton pieces meet). As undesired effect we get the presence of spurious patches on the scaffold that are not associated to any piece of the skeleton. Example of methods generating extra quads are those in [48]

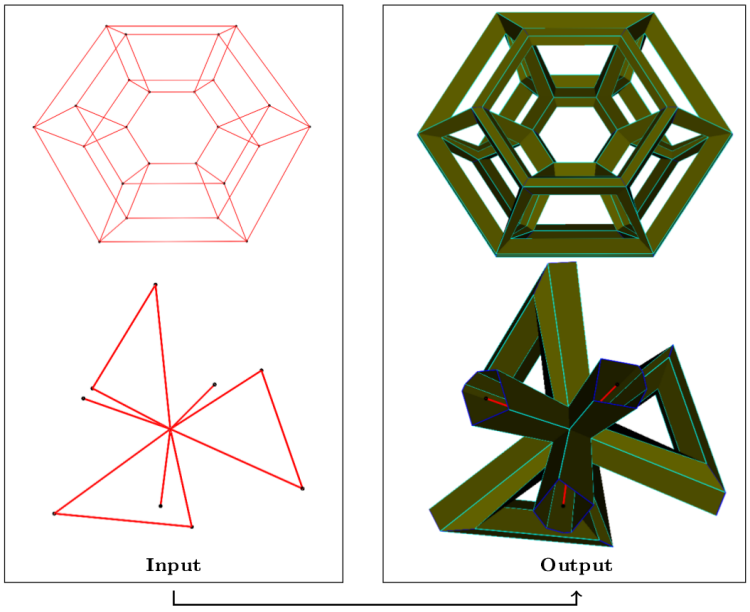

Figure 4.1: Scaffold construction.

and [49]. In [48, Figure 4] one can appreciate spurious quads around joints, while in [49, Figure 6] the extra quads are due to the presence of a cycle in the skeleton. In [46] the extra patches around joints are triangular patches, while [44] cannot handle skeletons with cycles.

In Chapter 1 of the thesis we present a method for generating scaffolds that can handle skeletons with cycles. Our method does not create spurious quads around joints, and allows to construct scaffolds that satisfy any group of symmetries of the input skeleton. We construct an optimal scaffold by minimizing the total number of quads in an Integer Linear Programming model, for which we formally prove feasibility. In Chapter 2 of the thesis we describe how to generate a hexahedral volumetric mesh from the scaffolds we construct. Avoiding spurious quads is not only useful for modeling and post-processes, but the total lack of spurious quads is a key property of our method that made possible the volumetric hexahedral meshing. Also in Chapter 2 we present a variant of our scaffolding method that would provide more control over the shape of the scaffolds.

Convolution surfaces. In skeleton-based modeling the user starts with a set of 1D (curves) or 2D (surfaces) objects that serves as skeleton for a shape surrounding it. Surfaces built around a skeleton are very useful since the skeleton provides an intuitive way to manipulate the surface. Several methods have been proposed for the generation of surfaces around 1D skeletons: sweep surfaces [52], offset surfaces [53], canal surfaces [54], B-Meshes [46], and convolution surfaces [55, 56, 57] are some of them. Convolution surfaces are specially attractive because they not only add radii information to the skeleton, but also provide a way to blend individual pieces in a smooth way (see Figure 4.2).

Convolution surfaces have been applied to tree modeling [58, 59], character modeling [60],

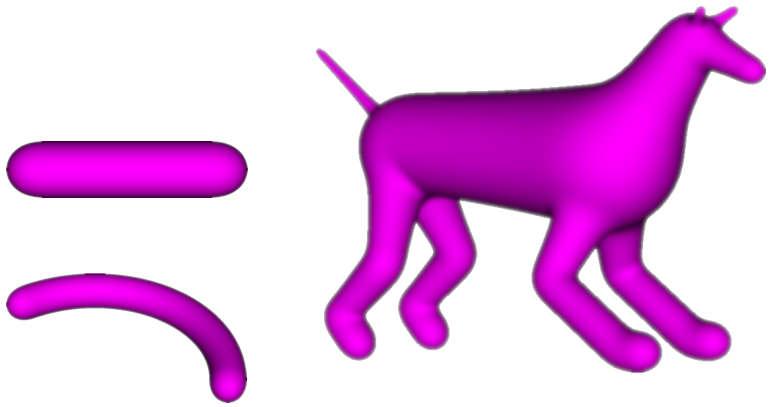

(a) Simple pieces. **(b)** Complex model.

Figure 4.2: Convolution surfaces

sketch-based modeling [61, 62, 63, 64], immerse modeling in virtual environments [65], and others. More specifically, a convolution surface is an implicit surface defined as a level set of a scalar field, the convolution field, that is obtained by integrating a kernel function over the skeleton. This technique can be used also to model volumes and are suitable to be combined in other implicit modeling frameworks [66, 67].

The mathematical smoothness of the surface obtained depends only on the smoothness of the kernel. The kernel function (power inverse, Cauchy, compact support, …) may be selected so as to have closed form expressions for the convolution functions associated to basic skeleton elements (line segments, triangles, …). The additivity property of integration makes the convolution function independent of the partition of the skeleton. More general skeletons are then partitioned and approximated by a set of basic elements. The convolution function for the whole skeleton is obtained by adding the convolution functions of the constitutive basic elements. See for instance [56, 68, 69, 70, 71, 72, 73, 74, 57, 75].

Line segments are the most commonly used 1D basic skeleton elements. When a skeleton consists of curves with high curvature or torsion, its approximation might require a great number of line segments for the convolution surface to look as intended. Arcs of circles form a very interesting class of basic skeleton elements in the context of convolution. This was already argued in [71] for planar skeleton curves. Indeed any space curve can be approximated by circular splines in a $\mathcal{G}^1$ fashion [76, 77]. A lower number of basic skeleton elements are then needed to obtain an appealing convolution surface, resulting in better visual quality at lower computational cost.

To model a wider variety of shapes it is necessary to vary the thickness around the skeleton. Several approaches have been suggested: weighted skeletons [78, 70, 72], varying radius [69], scale invariant integral surfaces [75], the latter two actually providing a more intrinsic formulation.

Closed form formulas, obtained through symbolic computation, have been the tool of

choice for evaluating the convolution fields. While general closed form formulas were obtained for weighted line segments in [78], there has been a lack of generality in terms of closed form formulas for convolution with varying radius, or scale, over line segments and, even more so, over arcs of circles. A study of the symbolic formulas for power inverse kernels is discussed in Chapter 4with the use of some advanced computer algebra techniques.

The recurrence formulas for arcs of circle with varying radii or scale present a formidable number of terms. Their numerical evaluation can lead to instabilities. We hence feel we pushed the symbolic approach to its limits. For a more versatile approach we call on numerical integration using the well established quadrature methods implemented in QUADPACK [79].

Anisotropy. Standard convolution surfaces around 1D skeletons have circular cross sections. That is also the case for varying radius and scale integral surfaces. This significantly restricts the shapes that can be generated. In Chapter 5 of the thesis we discuss previous approaches for mitigating this issue and we introduce a new technique to generate *anisotropic* convolution surfaces. A simple and intuitive approach to control the shape is also provided. In Figure 4.3 we illustrate anisotropy in the context of convolution surfaces.

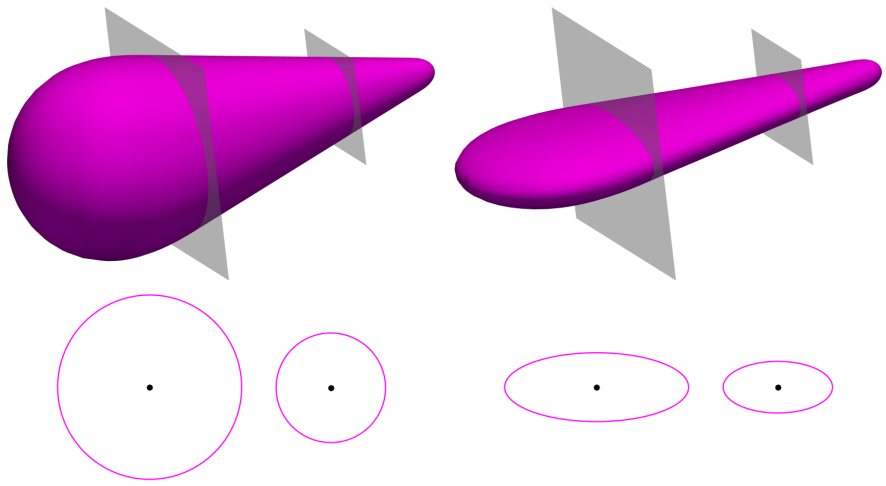

(a) Standard convolution. **(b)** Anisotropic convolution.

Figure 4.3: Anisotropy in convolution surfaces. In the top row we show the surface and two slicing planes. In the bottom we show the cross sections given by the slicing planes.

Medial axis, the most intrinsic skeleton, has 2D and 1D elements. Convolution surfaces around 2D skeletons have been approached in the literature [80, 81, 82, 63, 75, 65]. While useful, 2D skeletons increase the complexity in the formulas involved as well as on the modeling process for the user. In this thesis we favor the use of 1D skeletons. Anisotropic convolution limits the need of 2D parts by extending the capabilities of convolution around 1D skeletons such that one can mimic the effects of 2D skeletons, as discussed in Chapter 5 of the tehsis.

In this work we assume that the modeled surface is topologically consistent with the skeleton. The precise radii control introduced in Chapter 5 of the thesis allows the user to detect when this is not the case. Consistency between the surface and the skeleton allows to identify a good edge-flow on a surface mesh: when the edges "follow" the 1D skeleton. We explore in Chapter 5 of the thesis, after a brief discussion at the end of Chapter 1, the use of our scaffolds for the meshing of skeleton-consistent implicit surfaces with good edge-flow on the final mesh. For readers interested in a detailed discussion of skeleton-surface topological consistency in the context of convolution surfaces we refer to [83].

PySkelton. Our research results were implemented into a Python library. Our library makes use of established libraries for mathematical programming and numerical analysis: Qhull [84] for convex hull computations, GSL [85] and QUADPACK for numerical integration and root finding, and GLPK [86] for integer linear programming.

Much of the content of this work has been published and presented in the following papers and venues:

Scaffolding:

- [87] Fuentes Suárez, A. J. and Hubert, E. (2018b). Scaffolding skeletons using spherical Voronoi diagrams: Feasibility, regularity and symmetry. Computer-Aided Design, 102:83–93.

  Presented in SPM2018: Solid and Physical Modeling. June 11-13, 2018, Bilbao, Spain.

  Topic: full development of the scaffolding algorithm, generation of optimal quad-dominant meshes that respect the symmetries of the skeleton, and with the same number of patches around each line segment (*regularity*).

  Full content in Chapter 1 of the thesis.

- [88] Fuentes Suárez, A. J. and Hubert, E. (2017). Scaffolding skeletons using spherical Voronoi diagrams. Electronic Notes in Discrete Mathematics, 62:45–50.

  Presented in LAGOS2017: IX Latin and American Algorithms, Graphs, and Optimization Symposium. September 11-15, 2017, CIRM, Marseille, France.

  Topic: proof of feasibility for the construction of a scaffold (quad dominant mesh that follows the structure of the skeleton) for skeletons made of line segments of any topology.

  Extended abstract.

- Poster presentation: *Scaffolding skeletons using spherical Voronoi diagrams.* FoCM2017: Foundations of Computational Mathematics. July 10-19, 2017, Barcelona, Spain.

Convolution surfaces:

- [89] Fuentes Suárez, A. J., Hubert, E., and Zanni, C. (2019). Anisotropic convolution surfaces. Computers & Graphics, 82:106–116.

  Presented in SMI2019/IGS2019: Shape Modeling International 2019, International Geometry Summit 2019. June 17-22, 2019, Vancouver, Canada.

  Topic: An extension to the convolution surfaces technique that increases the modeling freedom. A scaffold-based meshing technique for implicit surfaces around a skeleton is also discussed.

  Full content in Chapter 5 of the thesis.

- [90] Fuentes Suárez, A. J. and Hubert, E. (2018a). Convolution surfaces with varying radius: Formulae for skeletons made of arcs of circles and line segments. In Research in Shape Analysis: WiSH2, Sirince, Turkey, AWM, pages 37–60. Springer.

  Topic: study of symbolic formulas for convolution surface fields, introduction of Creative Telescoping in the context of closed form formulas for convolution surfaces.

  Partial and adapted content in chapters 3 and 4 of the thesis.

- Poster presentation: *Anisotropic convolution for modeling 3D smooth shapes around 1D skeletons*. 9th International Conference on Curves and Surfaces. June 28-July 4, 2018, Arcachon, France.

As a summary, the contributions in this thesis are:

- Scaffolding algorithm and extensions.
- Anisotropic convolution surfaces.
- Meshing of implicit surfaces using scaffolding.
- Python library implementing scaffolding and anisotropic convolution.
- Symbolic integral formulas for convolution surfaces through recurrence.

Chapter 5

Jan Legerský: Flexible and Rigid Labelings of Graphs

One of the core questions of Rigidity Theory is the number of realizations of a graph in the plane or space such that the distances between adjacent vertices are equal to given edge labels. Since any rotation or translation of a realization yields another realization compatible with the same edge lengths, only non-congruent realizations are counted. A labeling is said to be *flexible* if the number of compatible non-congruent realizations is infinite, otherwise *rigid*. Figure 5.1 shows the 3-prism (Desargues) graph illustrating that a graph might have both a flexible and a rigid labeling. Notice that the flexible labeling of the 3-prism is very specific — the triangles are congruent and the vertical bars have the same length. A graph is called *generically rigid* if the labeling obtained by measuring the distances of adjacent vertices in a generic realization is rigid. The main focus of this thesis is on flexible, necessarily non-generic, labelings of generically rigid graphs in the plane. Besides that, we study also rigid instances with many real realizations both in the plane and space.

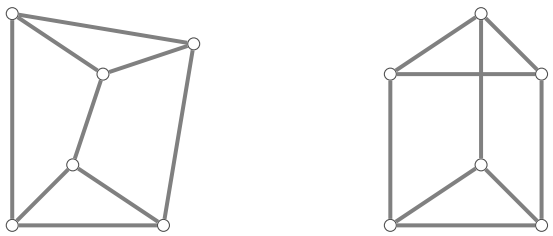

Figure 5.1: The 3-prism graph with a rigid (left) and flexible (right) labeling. The upper triangle can move along a circle in the flexible case.

A graph with a flexible labeling in the plane can be viewed as a planar linkage — the vertices represent rotational joints connecting links corresponding to the edges. A linkage moves paradoxically if the underlying graph is generically rigid. At the end of the 19-th century, Dixon [91] gave two constructions making the complete bipartite graph $K_{3,3}$ flexible (see also [92, 93]). The first construction gives a flexible labeling by placing the vertices of

each part on one of the two orthogonal lines. In the second one, the vertices lie in the corners of two concentric rectangles with perpendicular/parallel sides, see Figure 5.2. Also other examples like Burmester's focal point mechanism [94] or constructions by Wunderlich [95, 96] are known. For bipartite graphs, infinitesimal motions have been studied [97, 98] as well as the existence of a flexible labeling [99]. Walter and Husty [100] proved in 2007 using resultants that the constructions for $K_{3,3}$ given by Dixon are the only possible ones. In general, flexible labelings of individual graphs, resp. the class of bipartite graphs, were studied.

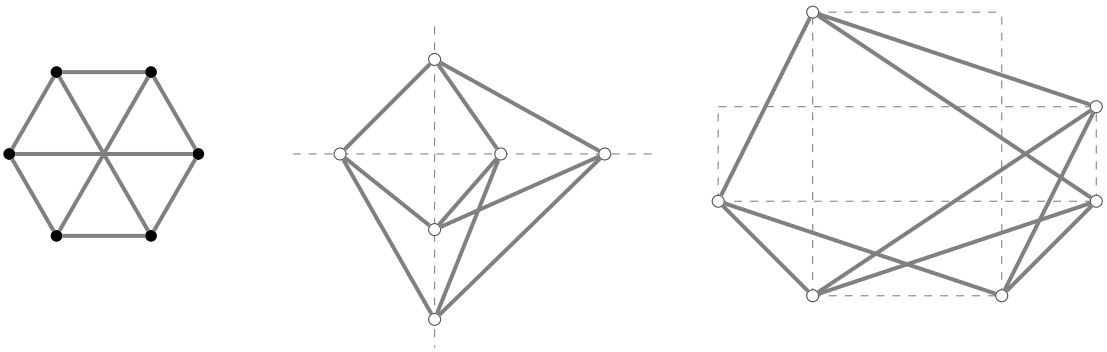

Figure 5.2: The complete bipartite graph $K_{3,3}$ (left) and Dixon's constructions of flexible labelings of $K_{3,3}$ (middle and right).

We aim to develop more general techniques. Our first result is the combinatorial characterization of the graphs that admit a flexible labeling. We prove that a graph has a flexible labeling if and only if it has a *NAC-coloring*. A NAC-coloring is a coloring of edges in red and blue such that for every cycle, either all edges have the same color or there are at least two edges of each color; Figure 5.3 gives two examples. A flexible labeling is constructed from a NAC-coloring by placing the vertices into a grid so that the edges do not create any diagonals. The other direction uses valuations of the function field of the curve of realizations compatible with a flexible labeling.

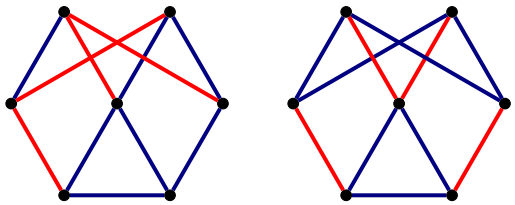

Figure 5.3: Two NAC-colorings of a graph.

We give a necessary condition on the existence of a NAC-coloring exploiting 3-cycles in the graph. We also show that certain vertex or edge cuts imply a NAC-coloring. We conjecture that the necessary condition is also sufficient for *minimally rigid* graphs in the

plane — a generically rigid graph is minimally rigid if the graph with any edge removed is not generically rigid. The conjecture is proved for a large subclass.

The realizations compatible with a flexible labeling coming from NAC-coloring are not always vertex-injective, namely, some nonadjacent vertices might coincide. A flexible labeling is called *proper* if there are infinitely many non-congruent vertex-injective realizations. Clearly, the over-constrained mechanisms mentioned above have a proper flexible labeling. We provide a necessary condition on the existence of a proper flexible labeling — a graph G can have a proper flexible labeling only if the graph obtained from G by adding some extra edges based on the NAC-colorings of G is not complete. We list all generically rigid graphs up to 8 vertices that satisfy the necessary condition. By various constructions, we prove that these graphs actually have a proper flexible labeling. Nevertheless, an example showing that the condition is not sufficient for an arbitrary number of vertices is given.

Next, we present tools for determining possible families of proper flexible labelings for a given graph G. A set of NAC-colorings of G can be assigned to a curve of realizations compatible with a flexible labeling. We propose a method determining such *active* NAC-colorings using 4-cycle subgraphs of G. Next, an active NAC-coloring satisfying a certain assumption imposes algebraic constraints on the labeling. We illustrate the methods by giving an alternative proof for the result of Walter and Husty [100] classifying the proper flexible labelings of $K_{3,3}$. We also apply the technique to obtain the classification of the proper flexible labelings of a 7-vertex generically rigid graph, which had not been known before, see Figure 5.4.

Regarding the rigid labelings, the precise number of non-congruent compatible realizations for a given minimally rigid graph in the plane or space have been investigated in recent years. For instance, Borcea and Streinu proved that the 3-prism has up to 24 realizations in the plane [101]. A common approach is to consider the complex solutions of the algebraic system describing the realizations. The number of complex solutions is bounded for instance by the mixed volume of the system. Then, one tries to find edge lengths maximizing the number of real solutions. This has been done for the minimally rigid graphs in the plane up to 7 vertices [101, 102]. In the space, the number of real realizations was settled for the minimally rigid graphs with 6 vertices [103]. Recently, a combinatorial algorithm counting the number of complex solutions in the plane was proposed [104]. The algorithm was used to compute the numbers for all minimally rigid graphs in the plane up to 12 vertices [105]. The same paper gives also the numbers for all minimally rigid graphs in the space up to 10 vertices via Gröbner basis computation.

Our contribution is the following — we specify edge lengths with many real solutions for minimally rigid graphs in the plane up to 10 vertices that have the maximum number of complex solutions among all minimally rigid graphs with the same number of vertices. The edge lengths are obtained by random sampling close to unit lengths. In the spatial case, we propose a sampling method inspired by coupler curves and the approach of [101]. We focus on the minimally rigid graph with 7, resp. 8, vertices that has the maximum number of solutions.

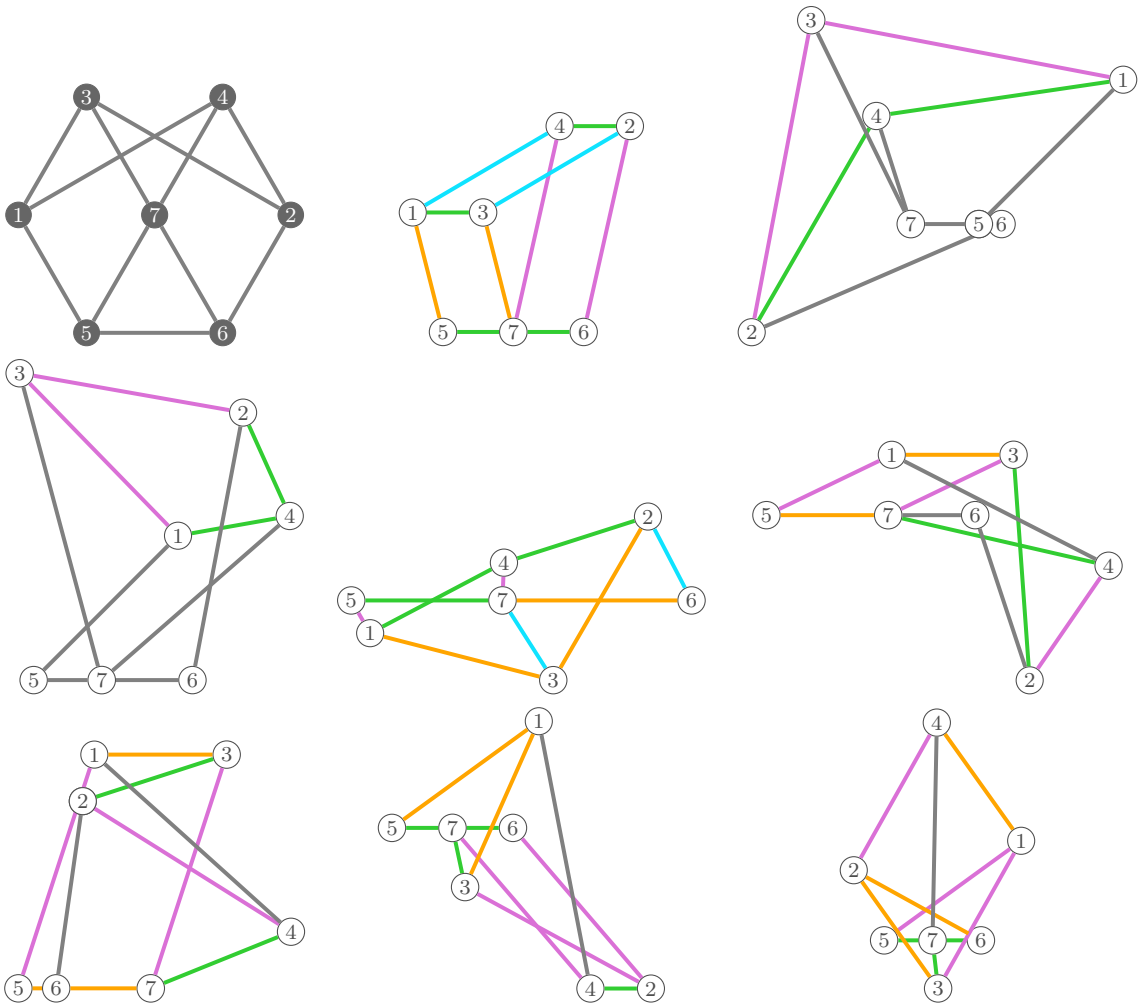

Figure 5.4: The graph in the top lef corner has 8 different families of edge lengths making it flexible. A representative of each if these families is depicted.

Using our implementation of the method, we obtained edge lengths such that the solutions for the 7-vertex graph are all real. For the graph on 8 vertices, we obtain edge lengths with many real realizations. Using known techniques for gluing graphs together [101, 105], we improve the asymptotic lower bounds on the number of real realizations.

The results of this thesis has been published by the author of the thesis together with Georg Grasegger and Josef Schicho [106, 107], resp. with Elias Tsigaridas, Vangelis Bartzos and Ioannis Emiris [108]. We remark that the papers [108, 107] were published after the defense of the thesis. Many concepts used in this thesis to study rigidity and flexibility in $\mathbb{R}^2$ are implemented in our package `FlexRiLoG` [109], which is written in `SageMath` [110] using object-oriented design. The methods dealing with realizations in $\mathbb{R}^3$ are implemented in another package [111].

Chapter 6

Francesco Patrizi: Refinement strategies and linear independence for LR-splines

Since the '70s, curves and surfaces in engineering have been usually expressed by means of Computer Aided Design (CAD) technologies, such as B-splines and Non-Uniform Rational B-splines (NURBS). These have numerous properties that allow to easily control and modify the geometries they describe:

- positivity,
- local supports,
- piecewise (rational) polynomials,
- partition of unity and convex hull property.

These properties make B-splines and NURBS useful tools to engineer objects with complex shapes. Furthermore, the introduction of Isogeometric Analysis (IgA) [112] has integrated such technologies into the Finite Element Analysis (FEA) as well, unifying the geometric description of the problem with its numerical resolution, in order to expedite the simulation process and gaining in accuracy. In addition to the properties listed above, B-splines and NURBS feature other qualities appreciated in this context, such as (local) linear independence and high global smoothness.

Nevertheless, the constantly increasing demand for higher precision in simulations and reverse engineering processes requires the possibility to refine only where large variations occur, in order to reduce the approximation error while retaining feasible computational costs. In order to achieve this adaptivity, new formulations of B-splines and NURBS have been established [113, 114, 115, 116, 117, 118, 119]. These new classes of functions are defined on locally refined meshes, in which T-vertices in the interior of the domain are

allowed, as opposed to classical B-splines and NURBS for which tensor meshes, with no internal T-vertices, are required.

Locally Refined B-splines, or in short LR B-splines [117], are one of these new formulations, and their definition is inspired by the knot insertion refinement process of B-splines. These latter are defined on global knot sequences, one per direction. In 2D, the insertion of a new knot in a knot sequence corresponds to a line segment in the mesh crossing the entire domain. This refines all the B-splines whose supports are crossed by the inserted segment. Instead, LR B-splines are defined on local knot vectors and the insertion of a new knot is always performed with respect to a particular LR B-spline. This means that in addition to the knot, one also decides which LR B-spline supports the corresponding line segment in the mesh is traversing, i.e., which LR B-splines have to be refined by the knot insertion. As a consequence, the LR B-spline definition is consistent with the B-spline definition when the underlying mesh at the end of the process is a tensor mesh, and the formulation of LR B-splines remains broadly similar to the standard B-splines even though they address local refinements. This makes them one of the most elegant extensions to achieve the adaptivity of the mesh and worthy of investigation.

LR B-splines satisfy the same properties of classical B-splines except the local linear independence for which a particular structure of the mesh is required. Even though such a characterization for the local linear independence of the LR B-splines in terms of meshing constraints is provided in [120], an adaptive refinement strategy to produce meshes with this structure was missing in the literature. To the best of my knowledge, the only mesh construction that leads to a locally linearly independent collection of LR B-splines is proposed in [120] as well. However, such a process cannot be recorded as an adaptive refinement because the regions to be refined and the maximal resolution, i.e., the sizes of the smallest cells in the domain induced by the mesh, have to be chosen a priori. The purpose of the third chapter of the thesis is to describe the first fully adaptive refinement ensuring the local linear independence of the LR B-splines. Such a property allows, inter alia, to design efficient quasi-interpolation schemes and to bound the band-width in the matrices produced by the numerical discretization of PDEs.

More generally, the set of LR B-splines can even be linearly dependent if no assumptions on the locally refined mesh are established. Although linear dependence is not a major issue for geometric design, it constitutes a difficulty when performing simulations in the IgA context, as it requires the resolution of singular linear systems to assemble the numerical approximation. As of today, there is no known characterization of the linear independence for LR B-splines. The second chapter of the thesis starts this analysis by looking at geometric necessary conditions for the mesh to have a linear dependence relation among the LR B-splines. In particular, it relates the linear dependence to the position of the T-vertices in the mesh and to the LR B-spline support inclusions. These observations allow also the computation of the minimal number of LR B-splines that can form a linear dependence relation. Such a lower bound (8 functions) turns out to be independent of the polynomial

bidegree used to define the LR B-splines and it is sharp, as shown by the examples contained in the paper where a linear dependence relation with exactly 8 LR B-splines is provided for any bidegree $(p_1, p_2) \neq (0,0), (1,0), (0,1), (1,1)$.

For some applications, e.g., reservoir modeling and biomedical engineering, the geometry of the problem is not directly established within the CAD system but it has to be modeled from the scanning of a physical object. A fundamental step to generate a spline surface approximation of the acquired data is what is called mesh parametrization. This establishes a bijective map between a triangular surface, which represents a first approximation of the data, and a parameter domain. Mesh parametrizations almost always introduce distortions in either the angles or the areas, which affect the quality of the final spline surface approximation. Therefore, it is crucial to define mesh parametrizations as similar as possible to isometries in order to reduce such distortions. For piecewise linear surfaces, such as the triangular surfaces, a strategy that has proved to be efficient for this purpose consists of expressing the image of the interior vertices of the triangulation in terms of the images of the surrounding vertices using generalized barycentric coordinates. In particular, the mean value coordinates turned out to be a successful and popular choice thanks to their simple and closed formula and the smoothness of the resulting mesh parametrization.

Generalized barycentric coordinates allow the construction of smooth functions that interpolate piecewise linear continuous data prescribed at the boundary of a polygon. One can then consider the more general problem of finding a smooth function that interpolates the value of any given continuous function at the boundary of a closed domain. The mean value coordinates have been extended to a transfinte mean value interpolant to address this problem in [121]. However, a proof of interpolation is provided in [121] only under strong conditions on the shape of the boundary, which exclude polygonal domains. The fourth chapter of the thesis provides an alternative proof for these cases that relies on the continuity of the given data.

Bibliography

[1] A. Pauly, "On the topological aspects of the theory of represented spaces," *arXiv e-prints*, Apr 2012.

[2] A. Pauly and F. Steinberg, "Comparing representations for function spaces in computable analysis," *CoRR*, vol. abs/1512.03024, 2015.

[3] I. Z. Emiris, C. Konaxis, and C. Laroche, "Implicit representations of high-codimension varieties," *Computer Aided Geometric Design*, vol. 74, p. 101764, oct 2019.

[4] L. Busé, C. Laroche, and F. Yıldırım, "Implicitizing rational curves by the method of moving quadrics," *Computer-Aided Design*, vol. 114, pp. 101–111, sep 2019.

[5] T. Sederberg and F. Chen, "Implicitization using moving curves and surfaces," in *Proceedings of SIGGRAPH*, vol. 29, pp. 301–308, 1995.

[6] D. Cox, T. W. Sederberg, and F. Chen, "The moving line ideal basis of planar rational curves," *Computer Aided Geometric Design*, vol. 15, no. 8, pp. 803–827, 1998.

[7] D. Cox, T. Sederberg, and F. Chen, "The moving line ideal basis of planar rational curves," *Computer Aided Geometric Design*, vol. 15, no. 8, pp. 803 – 827, 1998.

[8] F. Chen and W. Wang, "The μ-basis of a planar rational curve - properties and computation," *Graphical Models*, vol. 64, pp. 368–381, 02 2003.

[9] D. Cox, R. Goldman, and M. Zhang, "On the validity of implicitization by moving quadrics of rational surfaces with no base points," *J. Symbolic Comput.*, vol. 29, no. 3, pp. 419–440, 2000.

[10] T. Sederberg, R. Goldman, and H. Du, "Implicitizing rational curves by the method of moving algebraic curves," *Journal of Symbolic Computation*, vol. 23, no. 2-3, pp. 153–175, 1997.

[11] Y. Lai and F. Chen, "Implicitizing rational surfaces using moving quadrics constructed from moving planes," *J. Symbolic Comput.*, vol. 77, pp. 127–161, 2016.

[12] X. Jia, X. Shi, and F. Chen, "Survey on the theory and applications of μ-bases for rational curves and surfaces," *Journal of Computational and Applied Mathematics*, vol. 329, pp. 2–23, 2018. The International Conference on Information and Computational Science, 2–6 August 2016, Dalian, China.

[13] N. Song and R. Goldman, "μ-bases for polynomial systems in one variable," *Computer Aided Geometric Design*, vol. 26, no. 2, pp. 217–230, 2009.

[14] L. Busé and T. Luu Ba, "Matrix-based implicit representations of rational algebraic curves and applications," *Computer Aided Geometric Design*, vol. 27, no. 9, pp. 681–699, 2010.

[15] L. Busé, "Implicit matrix representations of rational bézier curves and surfaces," *Computer-Aided Design*, vol. 46, pp. 14–24, 2014. 2013 SIAM Conference on Geometric and Physical Modeling.

[16] T. Luu Ba, L. Busé, and B. Mourrain, "Curve/surface intersection problem by means of matrix representations," in *SNC Conference*, pp. 71–78, ACM Press, 2009.

[17] L. Busé and T. Luu Ba, "The surface/surface intersection problem by means of matrix based representations," *Computer Aided Geometric Design*, vol. 29, no. 8, pp. 579–598, 2012.

[18] W. Bruns and H. J. Herzog, *Cohen-Macaulay Rings*. Cambridge Studies in Advanced Mathematics, Cambridge University Press, 1998.

[19] H. Hong, Z. Hough, and K. I., "Algorithm for computing μ-bases of univariate polynomials," *Journal of Symbolic Computation*, vol. 80, pp. 844–874, 2017.

[20] D. Eisenbud, *Commutative algebra with a view toward algebraic geometry*, vol. 150 of *Graduate Texts in Mathematics*. New York: Springer-Verlag, 1995.

[21] N. Botbol, A. Dickenstein, and M. Dohm, "Matrix representations for toric parametrizations," *Computuer Aided Geometric Design*, vol. 26, no. 7, pp. 757–771, 2009.

[22] M. Dohm and S. Zube, "The implicit equation of a canal surface," *Journal of Symbolic Computation*, vol. 44, no. 2, pp. 111 – 130, 2009.

[23] L. Busé and J. Jouanolou, "On the closed image of a rational map and the implicitization problem," *Journal of Algebra*, vol. 265, no. 1, pp. 312–357, 2003.

[24] W. Fulton, *Intersection theory*. Ergebnisse der Mathematik und ihrer Grenzgebiete, Springer-Verlag, 1984.

[25] M. Chardin, S. D. Cutkosky, and Q. H. Tran, "Fibers of rational maps and jacobian matrices," *Journal of Algebra*, 2019.

[26] F. Russo and A. Simis, "On birational maps and jacobian matrices," *Mathematics Subject Classiccations*, vol. 126, 01 2000.

[27] A. Doria, S. Hassanzadeh, and A. Simis, "A characteristic-free criterion of birationality," *Advances in Mathematics*, vol. 230, no. 1, pp. 390 – 413, 2012.

[28] A. Kustin, C. Polini, and B. Ulrich, "The equations defining blowup algebras of height three gorenstein ideals," *Algebra Number Theory*, vol. 11, no. 7, pp. 1489–1525, 2017.

[29] A. Kustin, C. Polini, and B. Ulrich, "Rational normal scrolls and the defining equations of Rees algebras," *Journal für die reine und angewandte Mathematik (Crelles Journal)*, vol. 650, pp. 23–65, 2011.

[30] L. Busé, M. Chardin, and A. Simis, "Elimination and nonlinear equations of rees algebra," *Journal of Algebra*, vol. 324, pp. 1314–1333, 11 2009.

[31] A. Kustin, C. Polini, and B. Ulrich, "Rational normal scrolls and the defining equations of rees algebras," *Journal fur die Reine und Angewandte Mathematik*, vol. 2011, 01 2009.

[32] B. Ulrich and W. V. Vasconcelos, "The equations of rees algebras of ideals with linear presentation," *Mathematische Zeitschrift*, vol. 214, pp. 79–92, 1993.

[33] N. Botbol, L. Busé, and M. Chardin, "Fitting ideals and multiple points of surface parameterizations," *Journal of Algebra*, vol. 420, pp. 486–508, 2014.

[34] N. Botbol, "The implicit equation of a multigraded hypersurface," *Journal of Algebra*, vol. 348, no. 1, pp. 381–401, 2011.

[35] M. Chardin, "Implicitization using approximation complexes," in *Algebraic geometry and geometric modeling*, pp. 23–35, Springer, 2006.

[36] W. V. Vasconcelos, *Arithmetic of Blowup Algebras*. London Mathematical Society Lecture Note Series, Cambridge University Press, 1994.

[37] J. Herzog, A. Simis, and W. V. Vasconcelos, "Approximation complexes of blowing-up rings, ii," 1982.

[38] J. Herzog, A. Simis, and W. Vasconcelos, "Approximation complexes of blowing-up rings," *Journal of Algebra*, vol. 74, no. 2, pp. 466 – 493, 1982.

[39] M. Chardin, "Regularity of ideals and their powers," 10 2013.

[40] A. Tagliasacchi, T. Delame, M. Spagnuolo, N. Amenta, and A. Telea, "3D Skeletons: A State-of-the-Art Report," *Computer Graphics Forum*, vol. 35, no. 2, pp. 573–597, 2016.

[41] G. W. Hart, "Solid-segment sculptures," in *Mathematics and Art*, pp. 17–27, Springer Berlin Heidelberg, 2002.

[42] G. W. Hart, "Sculptural forms from hyperbolic tessellations," in *2008 IEEE International Conference on Shape Modeling and Applications*, IEEE, 2008.

[43] V. Srinivasan, E. Mandal, and E. Akleman, "Solidifying Wireframes," in *Bridges: Mathematical Connections in Art, Music, and Science 2004*, (Banf, Alberta, Canada), pp. 203–210, 2005.

[44] J. A. Bærentzen, M. K. Misztal, and K. Wełnicka, "Converting skeletal structures to quad dominant meshes," *Computers and Graphics*, vol. 36, no. 5, pp. 555–561, 2012.

[45] A. Panotopoulou, E. Ross, K. Welker, E. Hubert, and G. Morin, "Scaffolding a skeleton," in *Association for Women in Mathematics Series*, ch. 2, pp. 17–35, Springer International Publishing, 2018.

[46] Z. Ji, L. Liu, and Y. Wang, "B-Mesh: A modeling system for base meshes of 3D articulated shapes," *Computer Graphics Forum*, vol. 29, no. 7, pp. 2169–2177, 2010.

[47] J. Wu and L. Liu, "Generating quad mesh of 3d articulated shape for sculpting modeling," *Journal of Advanced Mechanical Design, Systems, and Manufacturing*, vol. 6, no. 3, pp. 354–365, 2012.

[48] C.-Y. Yao, H.-K. Chu, T. Ju, and T.-Y. Lee, "Compatible quadrangulation by sketching," *Computer Animation and Virtual Worlds*, vol. 20, no. 2-3, pp. 101–109, 2009.

[49] F. Usai, M. Livesu, E. Puppo, M. Tarini, and R. Scateni, "Extraction of the Quad Layout of a Triangle Mesh Guided by Its Curve Skeleton," *ACM Transactions on Graphics*, vol. 35, no. 1, pp. 1–13, 2015.

[50] M. Livesu, A. Muntoni, E. Puppo, and R. Scateni, "Skeleton-driven Adaptive Hexahedral Meshing of Tubular Shapes," *Computer Graphics Forum*, vol. 35, pp. 237–246, oct 2016.

[51] S. Casti, M. Livesu, N. Mellado, N. A. Rumman, R. Scateni, L. Barthe, and E. Puppo, "Skeleton based cage generation guided by harmonic fields," *Computers & Graphics*, 2019.

[52] A. G. Requicha, "Representations for rigid solids: Theory, methods, and systems," *ACM Computing Surveys*, vol. 12, no. 4, pp. 437–464, 1980.

[53] B. Pham, "Offset curves and surfaces: a brief survey," *Computer-Aided Design*, vol. 24, no. 4, pp. 223–229, 1992.

[54] M. Peternell and H. Pottmann, "Computing rational parametrizations of canal surfaces," *Journal of Symbolic Computation*, vol. 23, no. 2-3, pp. 255–266, 1997.

[55] J. F. Blinn, "A Generalization of Algebraic Surface Drawing," *ACM Transactions on Graphics*, vol. 1, no. 3, pp. 235–256, 1982.

[56] J. Bloomenthal and K. Shoemake, "Convolution surfaces," *ACM SIGGRAPH Computer Graphics*, vol. 25, no. 4, pp. 251–256, 1991.

[57] C. Zanni, *Skeleton-based Implicit Modeling & Applications*. PhD thesis, Université de Grenoble, 2013.

[58] X. Zhu, X. Jin, and L. You, "Analytical solutions for tree-like structure modelling using subdivision surfaces," *Computer Animation and Virtual Worlds*, vol. 26, no. 1, pp. 29–42, 2015.

[59] X. Zhu, X. Jin, and L. You, "High-quality tree structures modelling using local convolution surface approximation," *The Visual Computer*, vol. 31, no. 1, pp. 69–82, 2015.

[60] C. Zanni, E. Hubert, and M.-P. Cani, "Warp-based helical implicit primitives," *Computers & Graphics*, vol. 35, pp. 517–523, jun 2011.

[61] E. Entem, L. Barthe, M.-P. Cani, F. Cordier, and M. van de Panne, "Modeling 3d animals from a side-view sketch," *Computers & Graphics*, vol. 46, pp. 221–230, 2015.

[62] A. Bernhardt, A. Pihuit, M.-P. Cani, and L. Barthe, "Matisse: Painting 2D regions for Modeling Free-Form Shapes," in *Eurographics Workshop on Sketch-Based Interfaces and Modeling* (C. Alvarado and M.-P. Cani, eds.), The Eurographics Association, 2008.

[63] X. Zhu, X. Jin, S. Liu, and H. Zhao, "Analytical solutions for sketch-based convolution surface modeling on the GPU," *The Visual Computer*, vol. 28, no. 11, pp. 1115–1125, 2011.

[64] J. Wither, F. Boudon, M.-P. Cani, and C. Godin, "Structure from silhouettes: a new paradigm for fast sketch-based design of trees," *Computer Graphics Forum*, vol. 28, pp. 541–550, apr 2009.

[65] X. Zhu, L. Song, L. You, M. Zhu, X. Wang, and X. Jin, "Brush2Model: Convolution surface-based brushes for 3D modelling in head-mounted display-based virtual environments," *Computer Animation and Virtual Worlds*, vol. 28, no. 3-4, 2017.

[66] A. Pasko, V. Adzhiev, A. Sourin, and V. Savchenko, "Function representation in geometric modeling: concepts, implementation and applications," *The Visual Computer*, vol. 11, no. 8, pp. 429–446, 1995.

[67] B. Wyvill, A. Guy, and E. Galin, "Extending the CSG tree. Warping, blending and boolean operations in an implicit surface modeling system," *Computer Graphics Forum*, vol. 18, no. 2, pp. 149–158, 1999.

[68] M.-P. Cani and S. Hornus, "Subdivision-curve primitives: a new solution for interactive implicit modeling," in *Proceedings - International Conference on Shape Modeling and Applications, SMI 2001*, pp. 82–88, IEEE Computer Society, 2001.

[69] S. Hornus, A. Angelidis, and M.-P. Cani, "Implicit modeling using subdivision curves," *The Visual Computer*, vol. 19, no. 2, pp. 94–104, 2003.

[70] X. Jin and C.-L. Tai, "Analytical methods for polynomial weighted convolution surfaces with various kernels," *Computers & Graphics*, vol. 26, no. 3, pp. 437–447, 2002.

[71] X. Jin and C.-L. Tai, "Convolution surfaces for arcs and quadratic curves with a varying kernel," *The Visual Computer*, vol. 18, no. 8, pp. 530–546, 2002.

[72] X. Jin, C.-L. Tai, J. Feng, and Q. Peng, "Convolution surfaces for line skeletons with polynomial weight distributions," *Journal of Graphics Tools*, vol. 6, no. 3, pp. 17–28, 2001.

[73] A. Sherstyuk, "Interactive shape design with convolution surfaces," in *Proceedings Shape Modeling International 99. International Conference on Shape Modeling and Applications*, pp. 56–65, IEEE, 1999.

[74] A. Sherstyuk, "Kernel functions in convolution surfaces: a comparative analysis," *The Visual Computer*, vol. 15, no. 4, pp. 171–182, 1999.

[75] C. Zanni, A. Bernhardt, M. Quiblier, and M.-P. Cani, "SCALe-invariant integral surfaces," *Computer Graphics Forum*, vol. 32, no. 8, pp. 219–232, 2013.

[76] A. W. Nutbourne and R. R. Martin, *Differential geometry applied to curve and surface design*. John Wiley & Sons, 1988.

[77] X. Song, M. Aigner, F. Chen, and B. Jüttler, "Circular spline fitting using an evolution process," *Journal of Computational and Applied Mathematics*, vol. 231, no. 1, pp. 423–433, 2009.

[78] E. Hubert and M.-P. Cani, "Convolution surfaces based on polygonal curve skeletons," *Journal of Symbolic Computation*, vol. 47, no. 6, pp. 680–699, 2012.

[79] R. Piessens, E. de Doncker-Kapenga, C. W. Überhuber, and D. K. Kahaner, *Quadpack*. Springer Series in Computational Mathematics, Springer Berlin Heidelberg, 1983.

[80] J. McCormack and A. Sherstyuk, "Creating and rendering convolution surfaces," *Computer Graphics Forum*, vol. 17, no. 2, pp. 113–120, 1998.

[81] X. Jin, C.-L. Tai, and H. Zhang, "Implicit modeling from polygon soup using convolution," *The Visual Computer*, vol. 25, no. 3, pp. 279–288, 2008.

[82] E. Hubert, "Convolution surfaces based on polygons for infinite and compact support kernels," *Graphical Models*, vol. 74, no. 1, pp. 1–13, 2012.

[83] G. Ma and R. H. Crawford, "Topological consistency in skeletal modeling with convolution surfaces," in *Volume 3: 28th Computers and Information in Engineering Conference, Parts A and B*, pp. 307–315, ASME, 2008.

[84] C. B. Barber, D. P. Dobkin, and H. Huhdanpaa, "The Quickhull algorithm for convex hulls," *ACM Transactions on Mathematical Software*, vol. 22, no. 4, pp. 469–483, 1996.

[85] M. Galassi, J. Davies, J. Theiler, B. Gough, G. Jungman, P. Alken, M. Booth, F. Rossi, and R. Ulerich, *GNU Scientific Library*. No. Release 2.4, GNU, 2017.

[86] A. Makhorin, *GNU Linear Programming Kit - Reference Manual*. 2016. https://www.gnu.org/software/glpk/.

[87] A. J. Fuentes Suárez and E. Hubert, "Scaffolding skeletons using spherical Voronoi diagrams: Feasibility, regularity and symmetry," *Computer-Aided Design*, vol. 102, pp. 83–93, 2018.

[88] A. J. Fuentes Suárez and E. Hubert, "Scaffolding skeletons using spherical Voronoi diagrams," *Electronic Notes in Discrete Mathematics*, vol. 62, pp. 45–50, 2017.

[89] A. J. Fuentes Suárez, E. Hubert, and C. Zanni, "Anisotropic convolution surfaces," *Computers & Graphics*, vol. 82, pp. 106–116, 2019.

[90] A. J. Fuentes Suárez and E. Hubert, "Convolution surfaces with varying radius: Formulae for skeletons made of arcs of circles and line segments," in *Research in Shape Analysis: WiSH2, Sirince, Turkey*, AWM, pp. 37–60, Springer, 2018.

[91] A. Dixon, "On certain deformable frameworks," *Messenger*, vol. 29, no. 2, pp. 1–21, 1899.

[92] W. Wunderlich, "On deformable nine-bar linkages with six triple joints," *Indagationes Mathematicae (Proceedings)*, vol. 79, no. 3, pp. 257–262, 1976. doi:10.1016/1385-7258(76)90052-4.

[93] H. Stachel, "On the flexibility and symmetry of overconstrained mechanisms," *Philosophical Transactions of the Royal Society of London A: Mathematical, Physical and Engineering Sciences*, vol. 372, 2013. doi:10.1098/rsta.2012.0040.

[94] L. Burmester, "Die Brennpunktmechanismen," *Zeitschrift für Mathematik und Physik*, vol. 38, pp. 193–223, 1893.

[95] W. Wunderlich, "Ein merkwürdiges Zwölfstabgetriebe," *Österreichisches Ingenieur-Archiv*, vol. 8, pp. 224–228, 1954.

[96] W. Wunderlich, "Mechanisms related to Poncelet's closure theorem," *Mechanisms and Machine Theory*, vol. 16, pp. 611–620, 1981. doi:10.1016/0094-114X(81)90067-7.

[97] E. Bolker and B. Roth, "When is a bipartite graph a rigid framework?," *Pacific Journal of Mathematics*, vol. 90, no. 1, pp. 27–44, 1980. doi:10.2140/pjm.1980.90.27.

[98] W. Whiteley, "Infinitesimal motions of a bipartite framework," *Pacific Journal of Mathematics*, vol. 110, no. 1, pp. 233–255, 1984. doi:10.2140/pjm.1984.110.233.

[99] H. Maehara and N. Tokushige, "When does a planar bipartite framework admit a continuous deformation?," *Theoretical Computer Science*, vol. 263, no. 1–2, pp. 345–354, 2001. doi:10.1016/S0304-3975(00)00254-1.

[100] D. Walter and M. Husty, "On a nine-bar linkage, its possible configurations and conditions for paradoxical mobility," in *12th World Congress on Mechanism and Machine Science, IFToMM 2007*, 2007.

[101] C. S. Borcea and I. Streinu, "The Number of Embeddings of Minimally Rigid Graphs," *Discrete and Computational Geometry*, vol. 31, p. 287–303, 2004. doi:10.1007/s00454-003-2902-0.

[102] I. Z. Emiris and G. Moroz, "The assembly modes of rigid 11-bar linkages," *IFToMM 2011 World Congress, Jun 2011, Guanajuato, Mexico*, 2011.

[103] I. Emiris, E. Tsigaridas, and A. Varvitsiotis, "Mixed volume and distance geometry techniques for counting Euclidean embeddings of rigid graphs," *Distance Geometry: Theory, Methods and Applications*, pp. 23–45, 2013. doi:10.1007/978-1-4614-5128-0_2.

[104] J. Capco, M. Gallet, G. Grasegger, C. Koutschan, N. Lubbes, and J. Schicho, "The Number of Realizations of a Laman Graph," *SIAM Journal on Applied Algebra and Geometry*, vol. 2, no. 1, pp. 94–125, 2018. doi:10.1137/17M1118312.

[105] G. Grasegger, C. Koutschan, and E. Tsigaridas, "Lower Bounds on the Number of Realizations of Rigid Graphs," *Experimental Mathematics*, pp. 1–12, 2018. doi:10.1080/10586458.2018.1437851.

[106] G. Grasegger, J. Legerský, and J. Schicho, "Graphs with Flexible Labelings," *Discrete & Computational Geometry*, vol. 62, no. 2, pp. 461–480, 2019.

[107] G. Grasegger, J. Legerský, and J. Schicho, "Graphs with Flexible Labelings allowing Injective Realizations," *Discrete Mathematics*, vol. in press, 2019.

[108] E. Bartzos, I. Z. Emiris, J. Legerský, and E. Tsigaridas, "On the maximal number of real embeddings of minimally rigid graphs in $\mathbb{R}^2$, $\mathbb{R}^3$ and S^2," *Journal of Symbolic Computation*, vol. in press, 2019. doi:10.1016/j.jsc.2019.10.015.

[109] G. Grasegger and J. Legerský, "FlexRiLoG — `SageMath` package for Flexible and Rigid Labelings of Graphs." Zenodo, May 2019. doi:10.5281/zenodo.3078758.

[110] The Sage Developers, *SageMath, the Sage Mathematics Software System (Version 7.5.1)*, 2017. `https://www.sagemath.org`.

[111] E. Bartzos and J. Legerský, "Graph embeddings in the plane, space and sphere — source code and results." Zenodo, 2018. doi:10.5281/zenodo.1495153.

[112] T. J. R. Hughes, J. A. Cottrell, and Y. Bazilevs, "Isogeometric analysis: CAD, finite elements, NURBS, exact geometry and mesh refinement," *Computer Methods in Applied Mechanics and Engineering*, vol. 194, no. 39-41, pp. 4135–4195, 2005.

[113] D. R. Forsey and R. H. Bartels, "Hierarchical b-spline refinement," *ACM Siggraph Computer Graphics*, vol. 22, no. 4, pp. 205–212, 1988.

[114] C. Giannelli, B. Jüttler, and H. Speleers, "Thb-splines: The truncated basis for hierarchical splines," *Computer Aided Geometric Design*, vol. 29, no. 7, pp. 485–498, 2012.

[115] T. W. Sederberg, J. Zheng, A. Bakenov, and A. Nasri, "T-splines and t-nurccs," in *ACM Transactions on Graphics*, vol. 22, pp. 477–484, ACM, 2003.

[116] A. Buffa, D. Cho, and G. Sangalli, "Linear independence of the t-spline blending functions associated with some particular t-meshes," *Computer Methods in Applied Mechanics and Engineering*, vol. 199, no. 23-24, pp. 1437–1445, 2010.

[117] T. Dokken, T. Lyche, and K. F. Pettersen, "Polynomial splines over locally refined box-partitions," *Computer Aided Geometric Design*, vol. 30, no. 3, pp. 331–356, 2013.

[118] J. Deng, F. Chen, X. Li, C. Hu, W. Tong, Z. Yang, and Y. Feng, "Polynomial splines over hierarchical t-meshes," *Graphical models*, vol. 70, no. 4, pp. 76–86, 2008.

[119] N. Engleitner and B. Jüttler, "Patchwork b-spline refinement," *Computer-Aided Design*, vol. 90, pp. 168–179, 2017.

[120] A. Bressan and B. Jüttler, "A hierarchical construction of lr meshes in 2d," *Computer Aided Geometric Design*, vol. 37, pp. 9–24, 2015.

[121] C. Dyken and M. S. Floater, "Transfinite mean value interpolation," *Computer Aided Geometric Design*, vol. 26, pp. 117–134, 2009.